Motion artefact reference sensor study for ECG signals

by

Anirudh Bisht

to obtain the degree of Master of Science
at the Delft University of Technology,
to be defended publicly on Thursday September 27, 2018 at 12:30 PM.

Student number:	4624246	
Project duration:	November 16, 2017 – September 27, 2018	
Thesis committee:	Prof. dr. PJ French,	TU Delft, supervisor
	Prof. dr. ir. WA Serdijn,	TU Delft
	Mr. Mario Konijnenburg,	Imec, daily supervisor
	Dr. ir. A. Bossche,	TU Delft
	Mr. Tom Torfs	

This thesis is confidential and cannot be made public until September 30, 2020.

TU Delft

Preface

I would like to thank Prof. Paddy French for guiding me through my thesis and being patient with me as I took my time in reaching my goals. I would like to thank both my supervisors at Imec Mario Konijnenburg and Tom Torfs for continously monitoring and guiding me through this thesis. Mario Konijnenburg, I would like to thank for ensuring I had always had the resources I needed to work, and helping with particularly challenging points during the project. Tom Torfs, I would like to thank for sharing his knowledge of analog systems, and the many ideas and tips that were crucial to this project.

I would like to thank my parents for their continious support through my life and especially so during this thesis. I am truly grateful that you always believe in me, and enourage me to pursue my dreams. I would like to thank my brother for his useful tips and for being an insipiring role model, I attempt to emulate you everyday in my life.

Finally I would like to thank all the people I have met and befriended during my stay here in The Netherlands, your stories are the ones that will always stay with me.

Anirudh Bisht
Eindhoven, September 2018

Contents

Abbreviations

AC Alternating Current

AFib Atrial Fibrillation

AHB Advanced Microcontroller Bus Architecture (AMBA) High-performance Bus

AMBA Advanced Microcontroller Bus Architecture

APB Application Peripheral Bus

BIOZ Bio Impedance

CMSIS Cortex Microcontroller Software Interface Standard

CPI Counts Per inch

CS Chip Select

CSV Comma-Seperated Values

DC Direct Current

DMA Direct Memory Access

DRL Driven Right Leg

DSP Digital Signal Processor

ECG Electrocardiogram

FFT Fast Fourier Transform

GPIO General Purpose Input Output

GSR Galvanic Skin Response

GUI Graphical User Interface

I2C Inter-Integrated Circuit

IC Integrated Circuit

LED Light Emitting Diode

MAR Motion Artefact Reference system

MUSEIC V2 Multi Sensor Integrated Circuit V2

NVIC Nest Vector Interrupt Controller

PCB Printed Circuit Board

PLL Phase Locked Loop

PPG Photoplethysmography

RAM Random Access Memory

SNR Signal to Noise ratio

SPI Serial Peripheral Interface

SQI Surface Quality Indicator

SRAM Static Random Access Memory (RAM)

SROM Static Read Only Memory

UART Universal Asynchronous Receiver-Transmitter

List of Figures

List of Tables

1 Introduction

This Thesis is a cumilation of 10 months of research and development done to analyse and better understand Motion Artefacts in ECG . This work was performed at the Holst Center,Eindhoven with the Connected Health Solutions lab of IMEC and working with the non-contact ECG group at Leuven.

Connected health is an evolving concept of providing remote health monitoring that moves health diagnostics outside of hospitals. Connected health is enabled with the help of technologies in sensor design and networking. Always enabled health monitoring increases the amount of data that is generated for healthcare operatives to analyse. Therefore Connected health solutions usually develop hand in hand with software monitoring solutions that perform automatic diagnositics of measured data. Connected health solutions is therefore touted as a socitechnical model for future healthcare systems[17]

Various medical diagnostic tools have already seen a shift into the consumer market with the advent of fitness bands and smart watches[16]. ECG is also used in medical diagnostics and has yet to see widespread reach in consumer electronics and wearable technologies. The reason for this being that ECG daignostics can identify a wide range of Cardiovascular diseases in patients. Cardiovascular diseases are the most common cause of death world wide claiming more than 17.7 million lives worldwide every year. [8]. However diagnosing them usually requires analysis of the ECG of the patient. ECG measuring tools used in clinical setting have been confined to being measured in a controlled hospital environment and usually only for the duration of the visit. On the other hand ECG monitoring tools developed with an aim for long term monitoring suffer from Motion Artefacts.[21] Motion artefacts distort the morphological data of the ECG signal, this makes it difficult to use the data for doctors and automated system alike that depend on clean data to make analysis. Motion artefacts as the name suggests arise from motion, this is the relative motion occuring in a system that consists of a subject being mesured and the mesurment system. Due to this reason ECG measuring tools have a hard time finding applications in consumer electronics, to guarentee usable data under a wide range of conditions they might get used in.

This thesis approaches the problem of motion artefacts from a adaptive noise filtering perspective2.4 and is aimed at finding a sensor or group of sensor that will act as a reference signals for artefact noise. The aim is to research and implement sensors that can capture the underlying pehenomna of motion artefacts and conclude if a sensor can act as a good reference sensor to distinguish motion artefacts from ECG.

For the purpose of this thesis an ECG measuring system was developed that measured motion of the electrode alongside the ECG. This thesis will discuss the choice of these sensors, the design of the protoype system known as the Motion Artefact Reference System (MAR system) and the results from its validation testing.

1.1. Research Question

Motion artefacts can be filtered out of the ECG signal using adaptive filtering, this requires a reference signal. Such a reference signal needs to be highly correlated to the underlying physical phenomena that causes motion artefacts at the same time being uncorrelated to the ECG itself. The aim of the thesis is thus to study various sensors and their ability to correlate to motion artefacts.

So the research question can thus be formulated as this

“Which sensor or combination of sensors can be used as a reference signal for motion artefacts in electrocardiogram signals“

To achieve this the following goals have to be met

- Research and select sensors that can capture the motion between an electrode and subject.
- Design and develop a system that can monitor using these sensors alongside ECG.
- Validate if these senors indeed show correlation to the motion artefact noise.

1.2. Thesis Outline

This thesis is broken down into five chapters. This chapter introduces the topic of the thesis the goals it set out to accomplish.

Chapter two provides background into ECG and the theory of motion artefacts as described in the literature. Moreover we will delve into the inner workings of the sensors that were studied for the purpose of the thesis.

Chapter three Will describe the design of the prototype system known as MAR. It will give an overarching architectural view of the system and highlight the physical and circuit level design of the system.

Chapter four will discuss the firmware level design of the system.

Chapter five will showcase the measurment and results from this system. The system was tested on ten subjects at the Holst Center during an investigative study of the system. A discussion on the nature of various artefacts and the usefulness of each sensor.

Chapter six will be the final concluding chapter, a case will be made for the importance of this research and its importance for the future. A discussion of the results and their significance for ECG monitoring. Moreover there will suggestions for the future of this sytem and ackowledge improvenments that could be made.

2

Background

2.1. ECG Theory

Electrocardigraphy is a part of Electrophysiology a branch of medical science that deals with the study of electrical voltages and currents of the body. Electrocardiography has been developed over the years in the medical industry to understand the inner workings of the heart by measuring the electrical voltage changes that occur.

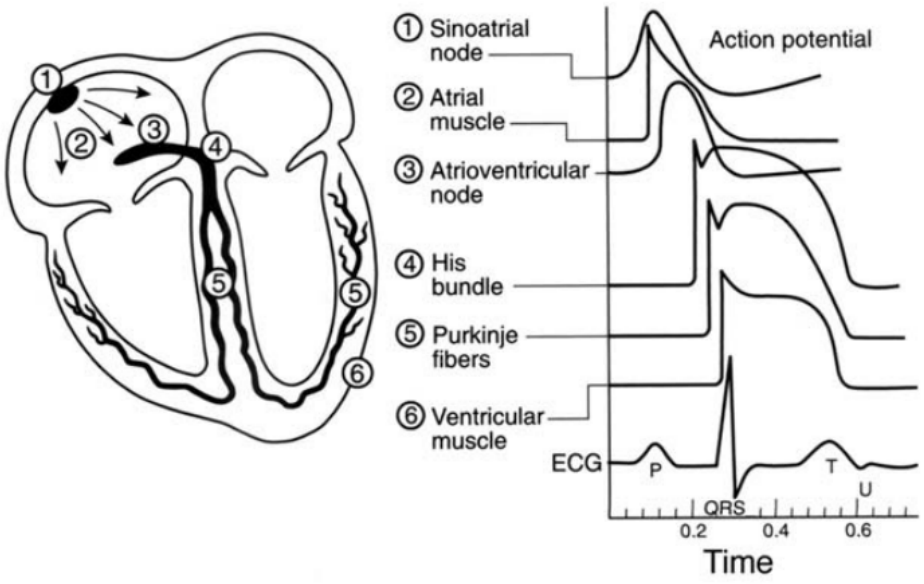

Figure 2.1: The activation stages of the heart. Taken from Fred M. Kusumoto's book ECG Interpertation `From Pathophysiology To Clinical Application`[29]

Activity of the heart mesured by the ECG is due to the polarisation and depolarisation of the cells during a cardiac cycle. 2.1 shows the standard PQRST wave assocaited with a single cycle of ECG and how differerent action potentials from the heart combine to form it. PQRST is the name given to the peaks that occur during a cardiac cycle, they are very distinct in their appearance and timing that they appear during the cardiac cycle. ECG holds information for diagnosing various heart condition based on both the morphological and temporal data of the ECG waveform.[33]

The morphological shape of the ECG signal comes due to the activation potential of the heart which is explained due to the polarization and depolarization of cells in different phases of a cariac cycle. The P wave is due to the depolarizion in the artrial chamber. The QRS complex which forms the most prominent peak in

a ECG curve is due to the depolarization of the much larger ventrical chamber. Finally the T wave is the result of the repolarization of the ventrical chamber. Since the artrial chamber is the smaller chamber of the heart the p wave is shorter than the QRS complex. Moreover depolarization of cells is a more rapid process than repolarization due to which the depolarization peaks have higher potentials[29].

In addition to the morpohological information, temporal information from the ECG curve gives information about the timings and rythm of the cardiac cycle. Temporal data in ECG that can be derived from visible PQRST parameters[29]

1. Heart rate: the rate of ventricular depolarization is measured as the time between adjacent QRS complexs, more accurately it is measured as the time between R peaks.

2. PR interval is measured from the beginning of the P wave to the begining of the QRS complex and corrosponds to the time between the artrial and ventrical activations. Normal value of PR interval in adults is 0.2s and is lower in babies

3. QT interval, measured from the start of the QRS complex to the end of T wave, it signifies the duration between the start and end of the ventricular phase. The QT interval is affected by the heart rate and becomes shorter as the heart rate goes up.

There are various heart conditions that can be diagonsed by monitoring the ECG. Abnormalities in the cardiac cycle are reffered to as arrhythmias. One of the arrythmias is Atrial Fibrillation (AFib). AFib is the irregular beating of the heart which arises due to problems in the artrial chamber.[14][38] AFib can be diagnosed by the presence of irregualr hertbeats, and presence of repeating P waves. [38]

Analysis of ECG signals for identifying arrythmias in a clinical environment is done by an expert by visual inspection of an ECG trace. There also exist algorithms for automating or semi-automating this process [20] moreover also possible is to use neural networks to perform this annotation [28].

2.1.1. ECG Electrodes

There are various types of electrodes used to observe ECG signals from the body.

Wet Gel Electrodes

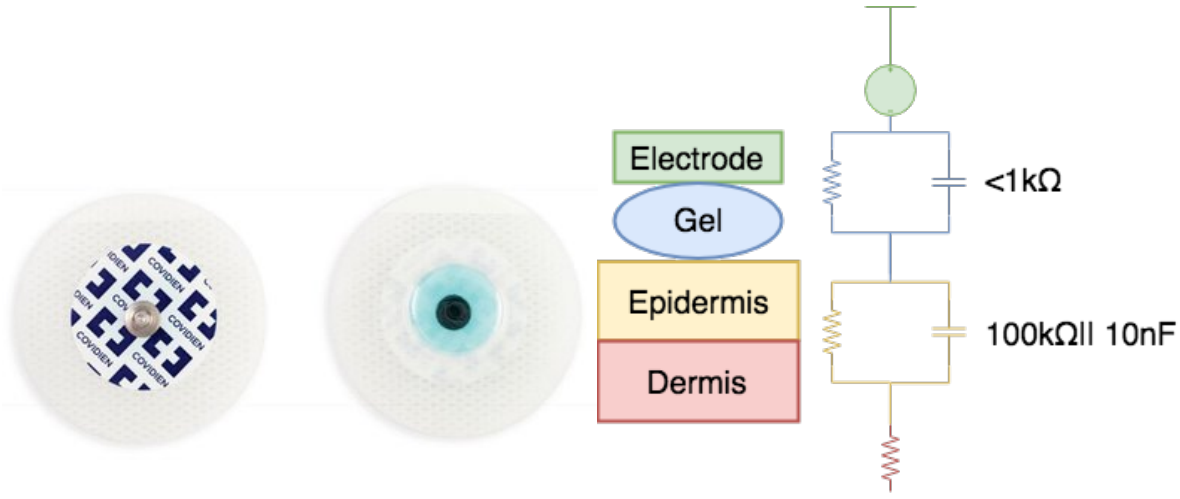

(a) a (b) b

Figure 2.2: Wet Gel or Ag Ag/Cl electrode (a) A wet gel electrode [4] (b) Equivalent circuit showing electrode skin coupling adapted from [19][25]

Wet Gel electrodes more precisely Silver Chloride Electrodes(Ag/AgCl) are current industry standard electrode and nearly all clinical ECG monitoring uses them[25]. Ag/Cl use a thin film of silver on electrode surface. The most important part is a gel of dissolved Cl- ions between the electrode and skin. This gel provides a continuous ionic contact with the skin by facilitating ion flow between the silver electrode and the skin. This property of Ag/Cl electrode makes them more resilient to motion artefacts compared to the dry-electrodes

and non-contact electrodes, since motions do not change impedance between the skin and electrode. There are however some disadvantages to Ag/Cl electrodes. Primarily use of Ag/Cl electrodes for long term monitoring causes deterioration in the Signal to Noise ratio (SNR) when the conductive gel evaporates [34]. Ag/Cl electrode also uses medical adhesive tape to hold the electrode in place, this requires skin preparation to remove body hair from the skin where measurements needs to be performed.

Dry-Contact Electrodes

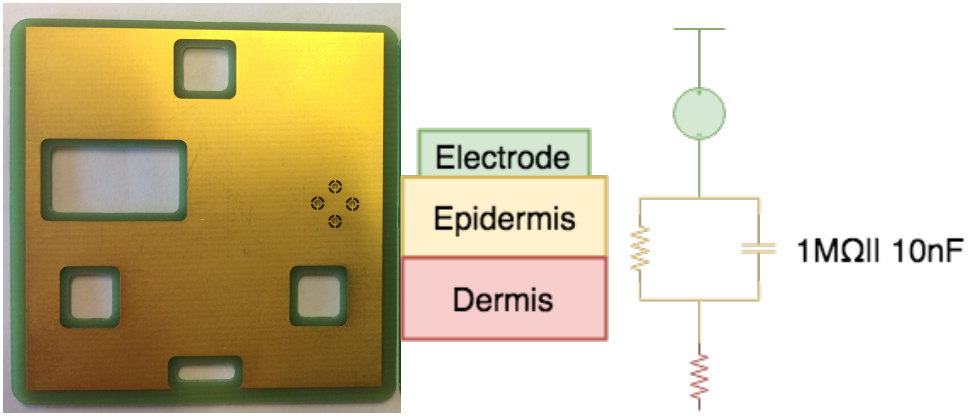

(a) a (b) b

Figure 2.3: A dry Contact electrode (a) electrode from MAR system (b) Equivalent circuit showing electrode skin coupling adapted from [19][25]

Dry contact electrodes make direct contact with the skin without the electrolyte medium. This removes the effects of the electrolytes that comes from drying up of electrolyte over time, and skin irritation that it causes. However removing the electrolytic medium makes the electrode-skin impedance variable and subject to motion noise. Presence of moisture trapped between the electrode and skin can bring down this impedance and drying of this moisture can bring it back creating more noise. [25]

Various other dry electrode structures have been proposed to reduce the noise caused by changing impedances. Variations of the standard dry electrode include. Textile based dry contact Electrodes[19] [15] Needle surface finsih, designed to be used with hairy skin surfaces which can be used witout the need for shaving the needle structure penetrates past the hairs to make direct contact with the skin.[36] Mesh surface dry electrode using carbon nanotubes mesh surface that forms a fine layer of contact [13]

Non-Contact Electrodes

Non-contact electrodes measure ECG through an capcitive coupling to the subject instead of a direct contact.[37][40] There is an insulating material present between the electrode and skin. The insulation provides capcitive coupling of the electrode to the skin 2.4 This allows non-contact electrodes to measure ECG through insulated materials like clothing. Non-contact electrodes are charchterized as having high input imedance buffers at the input. The design of the Non-contact electrode implemented for the purpose of this thesis is based on the imec non-contact group design. [40]. It uses active electrodes in the frontend that individually connect to a backend for signal processing and differential amplification.

DRL

For biasing the subject a Driven Right Leg (DRL) circuit is implemented. A DRL is circuit is used for removing common mode noise in ECG. Due to the presence of noise in the environment, primarily Alternating Current (AC) mains, the subject body will be coupled to this noise and the ECG signal being mesured can get drowned out.[44] Since this noise is present in both electrodes it can be removed as common mode noise. A DRL circuit mixes the two differential signals, amplifies and phase inverts the signal by 180 degrees and biases the body using the output signal. Due the inversion of the signal the common mode noise is surpressed. The gain of the DRL amplifier can be adjusted and increased when common mode noise in the environment is higher or decreased when it begins to saturate.

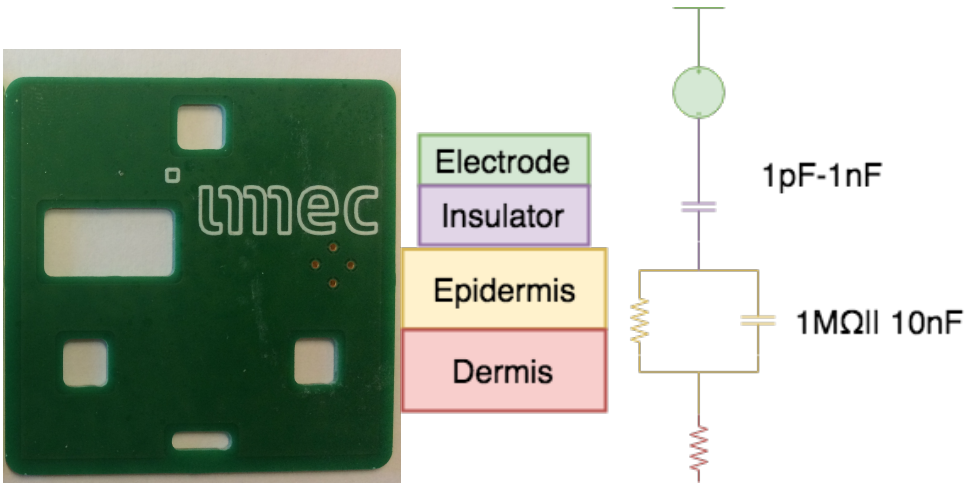

(a) a (b) b

Figure 2.4: A non-Contact electrode as implemented in MAR (a) non-contact electrode (b) Equivalent circuit showing electrode skin coupling adapted from [19][25]

2.2. Motion Artefact Theory

Motion artefacts have been studied as far back as 1984 [42]. While there have been many studies into various ways of reducing motion artefacts[24][21][18][41], few studies attempt to characterise and model the underlying phenomena that causes motion artefacts.

Generally there are two underlying pehenomena that are understood as the cause of motion artefacts. The first is attributed to the streatching of the skin under the electrode which in turn causes a change of voltage in the ECG measured signal.[43] The second is more applicable towards dry-contact and non-contact electrode and is attributed to the change in impedance between the electrode and skin. Wet-gel electrodes do not suffer from this impedance change due to the presence of the electrolytic gel that maintains an almost stable ionic contact between electrode and skin during their relative motion.[34]

Motion artefact is used as an umbrella term to reffer all noises that arise due to subject motions while recording ECG.

However there are many different motions that can occur between an electrode and skin system. An electrode that moves away from the skin will increase the impedance until ionic contact is lost. On the other hand an electrode that is pushed into the skin will stretch the skin and change its surface potential and cause artefacts of a different nature. Motion artefacts are easily noticed by humans while viewing an ECG signal. Computer algorithms running peak detection algorithms however have a harder time differentiating motion artefacts on ECG signals while evaluating them.[30] Motion artefacts in signal usually occur in band with the ECG signal, 2.5 shows the spectrum analysis of a typical ECG signal. As can be seen the T-wave occurs inband with motion artefacts, aggresive filtering of motion artefacts thus removes or distorts the morphological information of the T-wave and potentially other features of the ECG signal.

Motion artefacts also have a very dominant signal power over ECG which means that distortions caused by motion artefacts drown the ECG signal usually beyond recovery. It is due to this reason that a preffered way to deal with motion artefacts lies in rejecting the distorted signal rather than attempting to recover it.

Signals that can accurately indicate where the ECG signal will be distorted and hence rejected from further analysis is a way to deal with motion artefact noise. The loss of information from dropping these signals can be partly compensated by performing long term monitoring to increase the total data avilable for analysis. Since dry-contact and non-contact electrodes are designed for long term monitoring they naturally make good candidates.

Recovery of signal from adaptive filtering using a reference signal is another way to deal with motion artefact noise. However this requires a good candidate reference signal that will correlate well with motion but will not be correlated to the ECG signal. However due to overlapping bandwidth and large signal power that motion artefacts have, recovery of any ECG signal from these corrupted signals will have slight distortions. These distortions might make it unacceptable to use these signals for morphological analysis of the ECG[19].

Hence we can see that motion artefacts pose a unique problem in filtering ECG due their overlapping

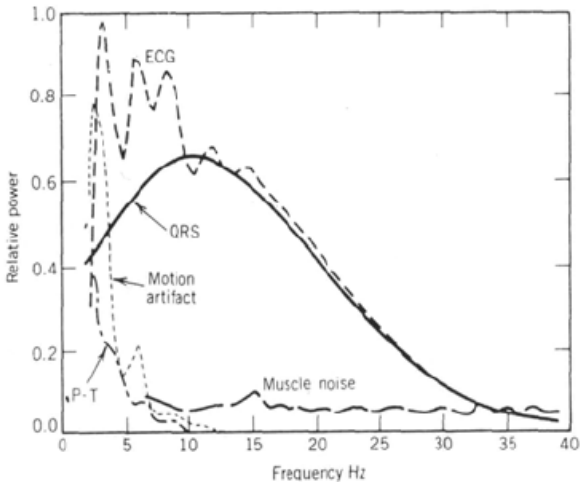

Figure 2.5: Spectral analysis of ECG and inband noise.[18]

bandwidth with the desired signal and high signal power.

2.3. Sensors Theory

To find a reference signal for motion artefacts the sensors considered were all off-the-shelf available sensors. The possiblity of a custom sensor design that might provide good correlation to the motion artefact noise has not been made part of this thesis, it however has been attemped in literature [32]. Instead we attempt to analyze the underlying physical phenomena as best we can to open research avenues for future desings. The aim of the thesis is to find reference signal, and attempt to validate, why the physical phenomena it measuers makes for a good refrence signal.

Sensors implemented have different theory of operation and measure different parameters, these parameters can be the intended use of the sensor or a derived use based on application. Some sensors were considered for this prototype but were later dropped from the final implementation due to the practical limitations in favour of readily available solutions. The sensors discussed are grouped by the physical phenomena they are measuring and highlighted in brief in 2.1.

Physical Phenomena	textbfSensor Name	textbfImplemented
Lateral Motion between electrode and skin	Optical Navigation sensor(PMW 3360)	Yes
Electrode Skin pressure	FSS005 Force sensor	Yes
Motion acceleartion of system	MPU-6050	Yes
Sub epidermal activity	Doppler Ultrasound	No pracitcal limitation on size of sensor
Distance between electrode and skin	Time of Flight Distance sensors	Limitation in accuracy of sensor
	DVRT or LVDT	No,power power requirenment
	Linear potentiometer	No,Noisy signal
	Laser Distance sensors	No,Size limitation

Table 2.1: Sensors considered and physical phenomena they measure

2.3.1. Optical Navigation Sensor

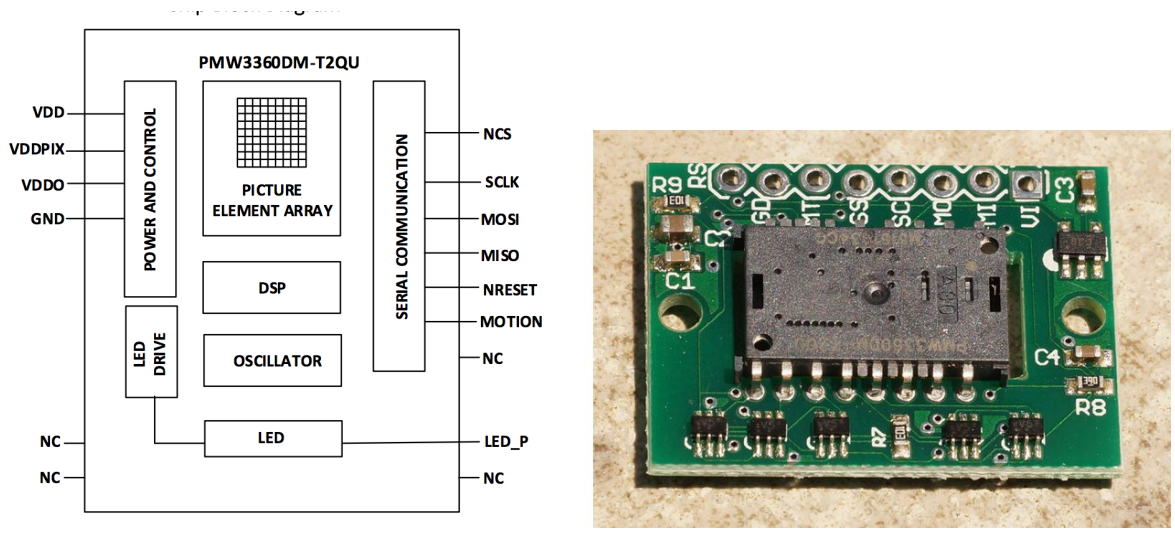

(a) a (b) b

Figure 2.6: (a) Functional block diagram of the Optical navigation sensor from datasheet of sensor[6] (b) Top view of sensor in evaluvation board

An optical navigation sensor is most commonly found in modern day computer mouse. It is used to measure two dimensional motion on the surface it is being used. Optical navigation sensor used in this project is a PMW3360 model from Pixart.

The principle of operation involves a LED used to illuminate a surface by the help of a lens to well illuminate the tracking surface. A optical sensor is used to capture the image of the tracking surface under the sensor using what is essentially a small camera of 128x128 pixels. This camera captures frames at a very high framerate and sends the data to an On-Chip Digital Signal Processor (DSP). The calculations performed on the DSP are first to extract features from the surface to track. These features are then tracked through successive images and their translation is used as an indication for the movement relative to the surface.

The sensitivity of the sensor is a digitally adjustable value called Counts Per inch (CPI), this value can be digital adjusted to best suit the situation in which the sensor is expected to perform. In addition to the displacement in X and Y axis there are additional parameters calculated by the DSP processor that are available to be used. These are the number of features that the DSP which is an indication of the surface quality. If a surface is smooth and clean there will not be many identifiable features for the DSP to track. This reduces the Tracking capability of the sensor.

Since the lens used in the sensor has a very short focal point lifting the sensor from the tracking surface reduces the number of visible features drastically. This in turn allows surface quality to act as a measure of the 'lift' or Z axis measure of the mouse sensor. This is used to by the modern mouse as a lift-cutoff parameter to stop tracking when the mouse has been lifted from the surface.

2.3.2. Force Sensor

Force sensor measure the force applied to part of the sensor. While there are many different principles of operation that can be applied to these sensors the most common method is to use piezoresistive strain gauge. Strain gauge measure the strain applied as a change in resistance. The change in resistance to the force applied is the pizeoresistive property of the sensor. This change in resistance can be read as an analog value, by making this resistance one arm of a whetstone bridge. The force sensor used in the MAR system uses the FSS005 series of force sensors by Honeywell that come in the described Whetsone bridge configuration.

2.3.3. Doppler Ultrasound

The Doppler Ultrasound finds its application as a consumer medical electronics product. Doppler Ultrasound Fetal monitoring are the products which allow pregnant women to hear the heartbeat of the fetus.

The doppler ultrasound works on the principal of the doppler effect. A wave of a given frequency when hitting a moving object will experience a shift from its original frequency. The shift in this frequency is played

back as a sound. Ultrasound frequency are chosen so as to achieve penetration through skin and reach a depth at which the fetus is present.

Measuring motion through a doppler allows for measuring of motion that is occuring deeper than the epidermal skin.

Doppler ultrasound sensor in an ECG electrode will allow us to view subepidermal motion and provide a unque insight. However ultrasound sensors that can achieve the depth of the epidermal layer reqiures frequencies in the range of 1-5Mhz. These cannot be easily implemented without the use of speacalised equipment and no easy to implment off-the-shelf solution exists and hence are not considered for this project.

2.3.4. Time of Flight Sensor

Time of Flight sensors measure distance to the target by measuring the time it takes for a photon to reflect off it. Timing resolution of Time of flight sensor directly affects its distance resolution.[7]

Compared to their optical distance measuring counterparts like Infra-red distance sensors, Time of flight sensors have better accuracy. While IR distance use intensity of reflected light as an indication of the distance, it can and is easily affected by ambient light and the reflectance of the surface. Time of flight senors are unaffected by the ambient lighting conditions and reflectance as long as the reflected light waves reaches back the distance will be accurate.

Time of flight sensor are available in easy to use packages which perform the illumination and reading of light and read out a digital value of the measured distance. While Time of Flight sesnor are easy to implement. However due to the strict requirements on timings required for short distances these sensors cannot produce the accuracy in the sub millimeter range. The VL530X by ST microelectronics in high performance mode has an accuracy of 3.5mm. The required distance resolution for this project was in the sub-mm range. This was determined in a previous study by measuring the capacitive changes due to air[40]. Hence Time of Flight sensor do not match the requirements and are not implemented.

2.3.5. DVRT

DVRT and their family of sensor like LVDT are industrial grade linear displacement sensors capable of very fine measurment over short distances usually 3-9 mm. Both LVDT and DVRT use the movenmet of a core in a coil and translate the induced current in the coil as a measure of distance. In a DVRT the coils are arranged in a half bridge Whetstone bridge configuration2.7. The differential voltage between VA and VB can be translated as the distance. In an LVDT the similar principle is followed but the AC excitation is towards the primary coil. LVDTs have an resolution as low as 300nm and an accuracy of 0.03mm. While the resolution and accuracy of DVRT make them suitable candiates for measuring electrode skin distance they fail in practicality of implementation due to the complexity of the signal conditioning required and high voltage AC signals required for their operations that make them less than idea to implement in biomedical environment. However they have been utilised by Hamilton et.al. [24] for measuring skin stretching.2.5.1

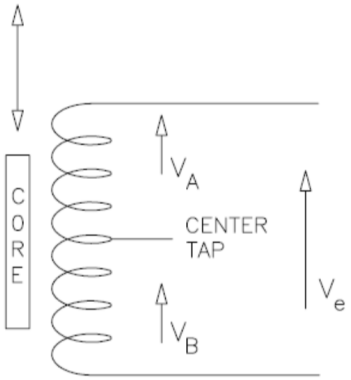

Figure 2.7: Circuit diagram of the DVRT functioning showing the moving coil, image taken from Lord Microstrain Websit[24]

2.3.6. Linear Potentiometer

Linear potentiometer measures displacement similar to a DVRT and LVDT, however it works on the principle of measuring distance using resistance changes. The working principle consts of a wiper arm that moves over a resistive film and shorts the resistance from the wiper position to the third contact. This translates the displacement to a resistance value. Measurment to this resistance can be made using either a constant current source or a whetstone bridge. However the movenment of the wiper over the resistive film causes disconnects during motion, this creates noise when the wiper is moving but gives steady results when held still. While measuring distance between an electrode and skin the breathing motion always keeps the linear potentiometer in motion and thus makes it unsuable for this system.

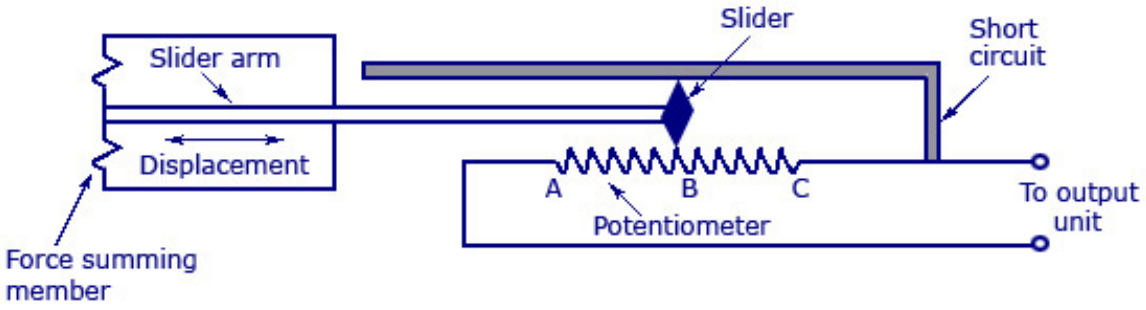

Figure 2.8: Circuit representation of Linear Potentiometer, Image taken from instrumentaiontoday.com [3]

2.3.7. Contact Microphone

Normal microphones are designed for picking up vibration from the air, contact microphone however are designed to be placed against a surface and measure its vibration. Contact microphone find use in recording from musical instruments and also for measuring bio signals. A contact microphone placed against the skin can measure small movenemnts as vibrations in the body including heart sounds .

These motion signals are shown to have correlation to noise in bio-potential signals by Velentin Goverdocsky et.al in [22]. The microphone used by them in the experiment has been carefully selected in regards to its plate displacement and sound hole to ensure that the measured signals were in the range of 2-50Hz making them suitable for capturing motion artefacts. Off-the-shelf contact microphones are more likely to be designed for musical instruments and hence have a different dynamic range that they respond to. This makes it difficult to implement a contact microphone suitable for measuring motion artefacts in this prototype. The custom microphone used by [22] was shown to have good correlation to motion artefacts and was used for motion artefact rejection.

2.4. Adaptive Filtering

Filters change the form of a signal based on some transfer function. Usually filters are used to remove frequencies in the signal above and below a certain range. These cut-off frequencies are determined by the parameters of these filters.

Adaptiving filters work on the principle of having variable filter parameters. These parameters can be varied with a reference signal to optimally remove noise. In the context of an adaptive filter an ideal reference signal is one that is perfectly correlates to the noise in the signal and is completely uncorrelated to the desired signal.

Hence for adaptive filtering motion artefact noise it will be desirable to find a reference signal that can correlate to the artefact noise. Since motion artefacts are tied to the relative motion between the electrode and the skin, the physical quantification of this motion will best capture the underlying phenomena and hence the motion artefacts.

Many approaches use accelerometer as reference signal for motion artefacts.[39] However this presents with two problems. The first is that not all motion motion artefacts can be captured by an accelrometer the stretching of the skin under the electrode will change the potential and hence ECG measured but cannot be captured by and accelerometer. Secondly accelerometer capture what can be described as system motion ie the motion of both the electrode and body. However the underlying cause of motion artefacts is in the relative motion between electrode and skin. Therefore a possible solution proposed for this is a mutli-sensor approach of multiple accelrometers, one can then measure the difference of the readings between them to estimate relative motion.[40] This approach however requires a study on the optimal placement of these sensors and development of mathematical tools to estimate the relative motion.

2.5. State of the Art

A literature study was done to understand the current ways in which motion artefact noise is handled. The most popular approach uses accelrometers to measure motion and use it as an reference signal in adaptive

filters.[35][27][26][31] While it is a popular approach this section will focus on the more novel sensors used in literature that attempt to measure skin stretching and lateral motion.

2.5.1. Skin Stretch

Measurenment of the skin stretch as a reference to the motion artefact noise in ECG has been discussed in the literature. For measuring skin stretch lots of sensors have been proposed, below we will discuss how some of these approaches measure the stretching of skin.

Skin stretching using DVRT

Patrick S Hamilton et.al. use a DVRT to measure skin stretching. [24] The DVRT is attached to a wet gel Ag-Ag/Cl electrode using metal barbs. since DVRTs can measure extremely fine motions the stretching of the flexible electrode is measurable by the DVRT. This implementation of a DVRT differs from the proposed method by this thesis, which planned to use them to measure absolute distance between the electrode and skin. However it is inline with the conclusion drawn that DVRT while extremely accurate, due to their prohibitively expensive cost, are not suited for a practical solution.

Skin stretch using light reflection

Nejet et.al propose a method for measuring the skin deformation using the property of polarising light.[23] While their method does not gear the results for use as a motion artefacts compensation method, the accuracy of measuring skin deformation makes that application a possiblity.

The working principle is that polarized light when reflecting off an surface undergoes scattering and random polarization. The amount of scattering and random polarization depends on the rougness of the surface. As the skin stretches it becomes smoother and hence a better reflector. Hence by measuring the change in polarization of light when reflecting of the skin will give an quantitative indication of skin stretching.

The measurment setup consists of a Helium-Neon laser which is passed through a light polariser. After undergoing polarising the light is reflected off the skin and measured by a photodetector after passing through a second parallel polariser. The two polarisers are parallel or perpendicular to each other in terms of angle of polarization and that only changes the interpretation of the output signal.

Since a highly coherent light source is required this method was not attempted to be recreated for this project

Optical stretch sensing

Yan Liu et.al. Implemented a optical sensor for measuring streatching of the skin. [31] While the paper does not go into details of describing the exact sensor, their description of the working principle of the sensor indicates it is an optical navigation sensor similar to the one discussed in 2.3.1. They implemeted the sensor into a Ag/Cl electrode and measured skin stretch. Calibration of the sensor was performed in-vitro on a sample of animal skin. They showed a linear realationship between the strain and the sensor displacement reading, having a correlatino coeicient of 0.9933.

Skin stretch using camera

Kalra et.al. implemented a method of quantifying skin stretching using a camera to image the skin. [12] The skin surface was inked with a checkeboard pattern, and a camera was used to capture a video of the skin under stretch. In post processing they analyzed frame by frame the movenment in the points of interest and quantified the skin stretching. The post processing used kalman filtering for denoising the ECG signal captured. This method is better in terms of using an optical navigation sensor because it gives more control over the choice of signal processing on raw data. In the optical navigation sensor the output is only availabel after the processing by the DSP. However the large pixel array limits the framerate possible and hence reduces the tracking accuracy.

2.5.2. Fexible Pressure Sensor

Luca et.al. implement an integrated wearable solution of ECG electrodes and pressure sensors in their paper [32]. The integrated design is implemented on a flexible PCB and implements a strain guage along with a electrode. The integrated design ensures co-location of measured signals of strain and ECG.

However while the paper does mention being able to record the ECG signal, they do not discuss motion artefacts and its relation to the motion signal they measure. Instead the motion signals are discussed as additional sensing for measuring muscle motion to understand bio-activity.

2.5.3. Lateral Motion

Tobias Wartzek et.al desiegned a custom capctive electrode that measured capcitive ECG in tandem with temperature and lateral motion[41]. This lateral motion measurenment was achieved by using a photodiode at the center of the electrode and a 3 of Light Emitting Diode (LED)s in a ring around it. The working principle is based on the fact that a moving body over the electrode will change the optical path of light reflecting back into photodiode. This principal can be used to quantify motion. The results used this lateral displacement as a Surface Quality Indicator (SQI) indicator for the ECG signal. As mentioned in the results the signal does not hold enough correlation to the artefact signal to achieve signal recovery.

3

Hardware Design

This chapter discusses the design of the MAR system from a hardware presepective It gives an outline of the envisioned system architecture and discuss in detail the physical and circuit level design. First we will discuss the system architecture, this will give an overview of how the system is designed and functions.

3.1. System Architecture

3.1.1. Overview

The MAR system design very much reflects its intention as a prototype system for testing a hypothesis. The system is not designed as an end-user product, it trades off portability in favour of rapid prototpying and easy access debugging.

The system has its core in the MUSEIC V2 chip from imec. The MUSEIC V2 is the second generation of imec's multi-signal acquisition Integrated Circuit (IC)s. It has been designed for low power usage, and since all data is acquired on one chip it is easy to synchronise data which is crucial if analysing the affect of one sensor against the ECG. The MUSEIC V2 was used in its evaluation board named Rose.

An overview diagram system architecture is shown in 3.1. The system is divided into two interconnected modules. The electrodes hence forth referred as the frontends are the ones that substitute normal ECG electrodes in this prototype. They contain a single buffered ECG electrode and all sensors required to monitor motion. Hence two of these electrodes in addition to a third passive bias electrode measure ECG in Lead 1 of the vertical plane or frontal leads of ECG.

The two electrodes individually connect to the backend system. The backend system performs signal acquisition in addition to various signal conditioning. The Rose board forms one half of the backend system, this includes the MUSEIC V2 and part of the power regulation. The other half is the backend system designed for this system.

When the system is used in non-contact mode the frontend circuit utilises a dual rail supply, this is generated by a virtual ground circuit in both the frontend and the backend. Connections between the electrodes and backend system are over a 30 pin Ribbon cable. The cable routes the power supply, digital signal lines, ECG , analog sensor lines and multiple ground lines for passive shielding.

3.1.2. Frontend Architecture

The frontend system is the term for the electrode in the MAR system. Each frontend comes in two variants namely non-contact and dry-contact. Each variant has one pair of electrodes. They differ in the ECG frontend circuit and the type of electrode PCB.

The sensors are shown along with the method of their communcation to the backend system in 3.2. The DVRT system is shown as a replacement module for one of the force sensors. The system has provisions to implement a DVRT sensor using a differential pair. Due to the bulky design and expensive component it is currently not implemented and hence shown faded. Similarly the PPG sensor is also shown faded. The PPG sensor is implemented on the dry contact electrodes. Due to high current in the LED sink creating noise on the board the sensors are disabled in the final implementation.

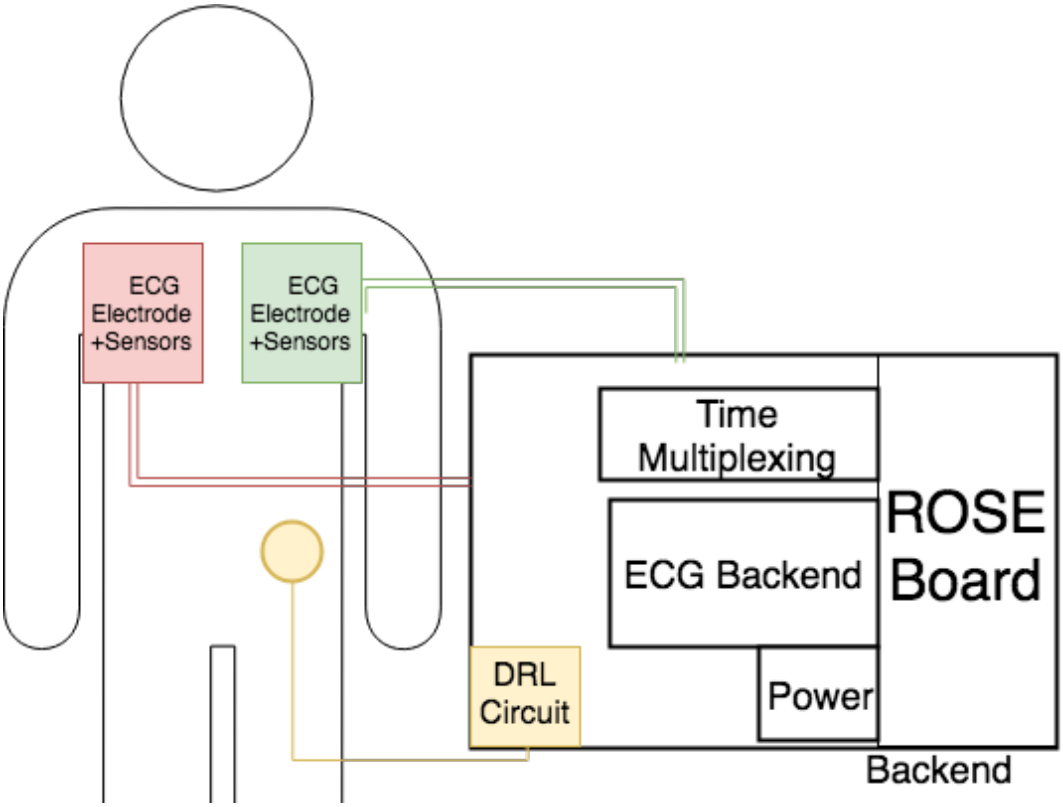

Figure 3.1: Overview of the overall system architecture.

3.1.3. Backend Architecture

The backend system is composed of two stacked PCBs. The bottom PCB is designed by imec and is the evaluvation board of their MUSEIC V2 ic.3.3 The top PCB has been designed as part of the MAR system. The connections made to the Rose board are to its IO ports.

The ports following the naming convention $N < number >$ are the General Purpose Input Output (GPIO) digital ports. The analog ports are named ANA_IO and are always in a differential pair. The digital signals are passed through to the Rose board, the Inter-Integrated Circuit (I2C) signals are level shifted to match the 1.8V tolerence of MUSEIC V2. The force sensors are stepped down from 3.3.V to 1.2V and multiplexed. This multiplexing is needed as there are six force sensors in the system and only three available analog channels on MUSEIC V2 to accomodate them.

A reference clock generated from MUSEIC V2 is used to synchronise the signals. This reference clock is derived from the 32Khz clock onboard that also acts as a reference to the MUSEIC V2 and its interal peripherals. The ECG signal on the backed is stepped down in a 10:1 ratio to make the 10V signal compatible with the 1.2V analog core of MUSEIC V2. Moreover the DRL circuit is used to bias the body when the system is used in non-contact mode.

Finally power managment circuitry manages the power supply from the battery, and a header switch allows switching to a bench power supply when testing the system.

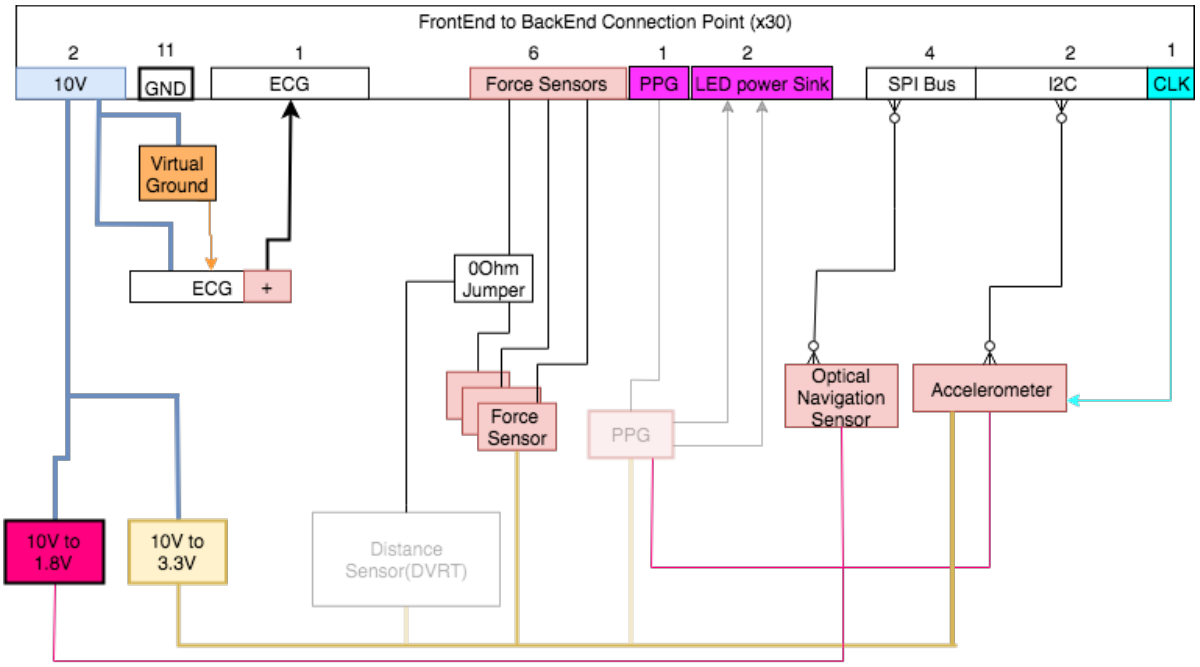

Figure 3.2: Frontend system architecture, showing the power distribution, sensors and backend connection setup. To note is the faded modules of PPG and DVRT that have provisions to be implemented but not actaully present.

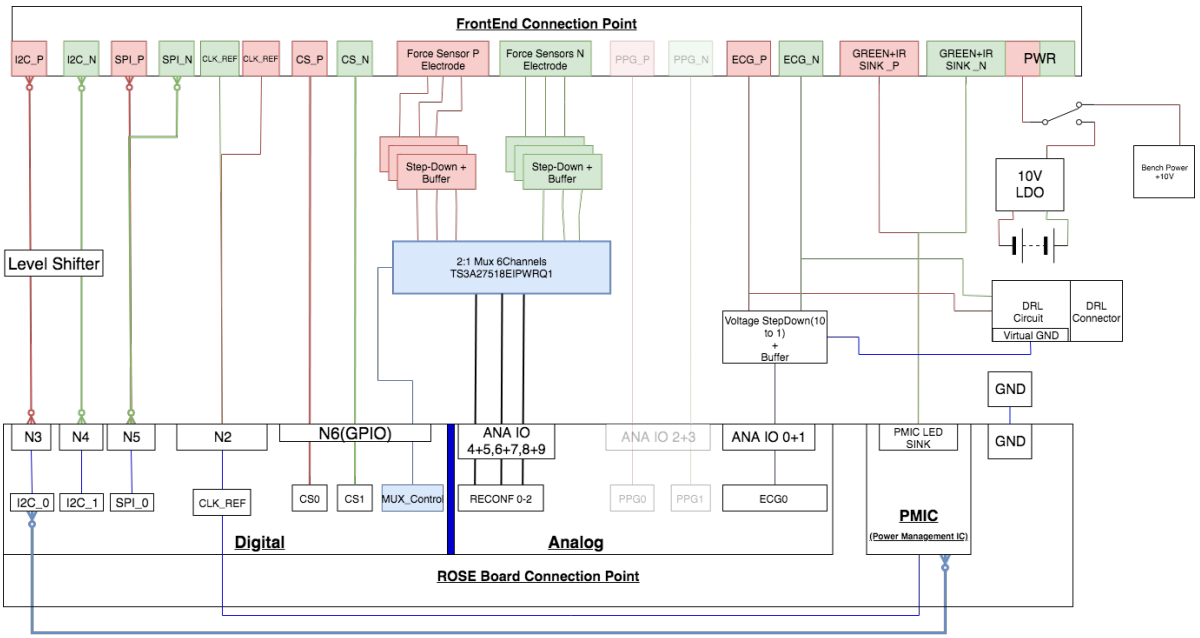

Figure 3.3: The backend system architecture, showing the multiplexing, power distribution, Connection to the frontend and connection to the Rose board.

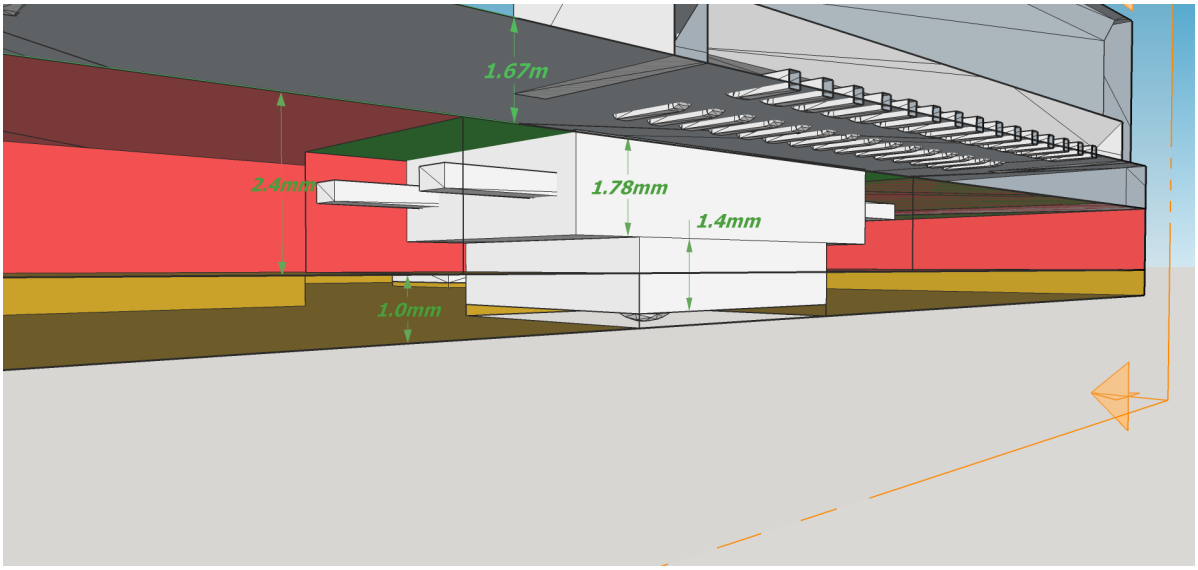

Figure 3.4: A sectional view of the 3D model of the MAR electrode. It shows the thickness of the three pcbs. The force sensor is placed at the bottom of Sensor PCB

3.2. Physical Design

The physical design of the prototype consists of two electrodes that have been designed to measure ECG and also motion signals in tandem with the ECG. Co-location of motion sensors and ECG is an important part of this physical design. As discussed by [22] and [40] co-location of the sensors and ECG electrode is vital in making correlations between motion signals and ECG. In the physical design of the electrode, all sensors measure the signals directly below the ECG electrode surface that is in contact with the skin.

Moreover a symmetrical design for the electrodes ensures that motion signals are measured on both electrodes independently.

The ECG frontend is implemented as three stacked PCBs, These three PCBs are referred as

- Electrode PCB. This comes in two variations for Non-Contact and Dry-Contact mode electrodes.
- Spacer PCB. Provides spacing for sensor discussed3.2
- Sensor PCB. Houses all the senors and connections to the backend system. While the PCB itself comes in a single version, the components soldered differ for dry-contact and non-contact electrodes.

The reason three stacked PCBs are used is to accomodate the sensors. The force sensor has a height of 3.1mm. To keep the measuring surface of the sensor flush against the flat electrode there needs to be spacing between where the sensor is soldered and the ECG electrode. This spacing is provided by the spacer PCB. With a combined thickness of 3.4mm the spacer PCB and electrode are thick enough to accomdate the force sensor in the stack as shown in the 3D model of the electrode in 3.4. Slots in the Spacer PCB and electrode PCB create cavities to accomodate these sensors.

Also to be accomodated is the optical navigation sensor, This is slightly more complicated due to the presence of a lens system in the optical navigation sensor. This lens sits in the cavity created by the spacer PCB.

The electrode PCB is the actual ECG electrode and thus is the bottom of the stack when the bottom faces the subject. This electrode has a two layers. The top layer provides a point to connect the bottom plate to the sensor electrode higher in the stack. This connection point is connected to the bottom measuring plate using vias. The top plate can be used as a guard plate in non-contact mode. There are two variants of this electrode. The Non-Contact electrode has the electrode plate covered by soldermask while the Dry-Contact variation has exposed metal(NiAu, nickle gold finish) contact. There are five slots in the Electrode PCB for the sensors. These are for the three force sensors that sit in a tripoint configuration one slot for the optical navigation sensor and a final slot for the disabled PPG sensor.

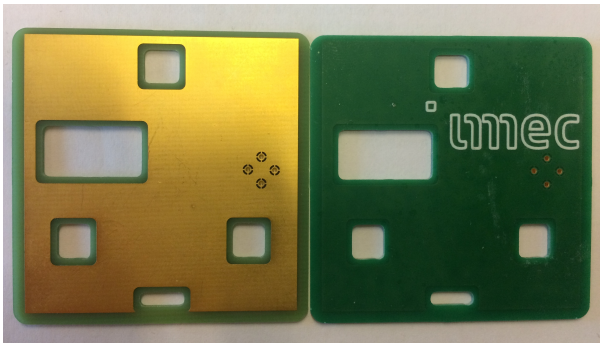

Figure 3.5: The bottom side of the two electrodes. The left is the dry-contact electrode with exposed metallic surface, with a Ni-Au finish. On the right is the non-contact with a soldermask finish.

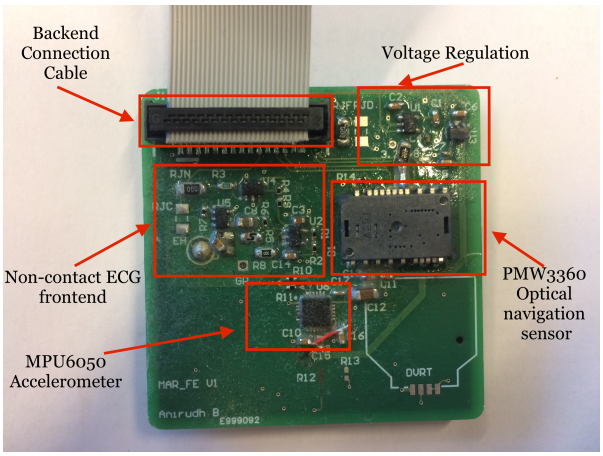

Figure 3.6: Top of the assembled electrode showing the sensor PCB and annotated to show the various sub-circuits and modules.

3.3. Circuit Design

3.3.1. MUSEIC V2 and Rose

MUSEIC V2 is implemented on the Rose evalulvation board by imec. The evaluvation board generates all the neccesary voltage levels for the MUSEIC V2 chip, in addition it has the imec deisgned Power Management IC(PMIC).

Also implmented is the CP2130 chip[2] to facilate communication between the music to a host PC. The CP2130 is a USB to SPI bridge controller and used to connect the Rose board to the host computer. MUSEIC V2 pins are exposed as 2.5mm pitch headers for the GPIO and MEDCAT connectors for the analog channels. The Backend board for MAR system is implemnted as a stackeable board on top of this taking insipiration from the stackable shields avaiable for the arduino platfoms.

The digital GPIO pins on the MUSEIC V2 are spilit into 8 groups of 4 pins each. Each group can be configured for a specific function including GPIO, I2C, SPI UART etc. These functionality is multiplexed internally to the different control blocks.

3.3.2. Power Regulation

The power requirenments for the system have a number of voltage level which are sourced differently on the frontend and backend. The voltages from the Rose board are generated using voltage regulators. The 10V is used by the frontend and backend to power the ECG circuits. The 5V is a mid-supply voltage from the virtual ground circuit. 3.3V is used by the Force sensors and I2C digital lines. 1.8V is the voltage level used by the optical navigation sensor and the connecting Serial Peripheral Interface (SPI) digital connection. 1.2V is the voltage of the analog core of the MUSEIC V2 and the highest voltage tolereated on its analog input pins.3.1 The ECG channels are therefore stepped down to this level.

Voltage	Source Backend	Source FrontEnd
10 V	Li-Ion battery or Bench supply	Backend
5 V	Voltage Divider	Voltage Divider
3.3 V	Rose Board	Voltage Regulator on Frontend
1.8 V	Rose Board	Voltage Regulator on Frontend
1.2 V	Rose board	Not required

Table 3.1: Voltage and power distribution

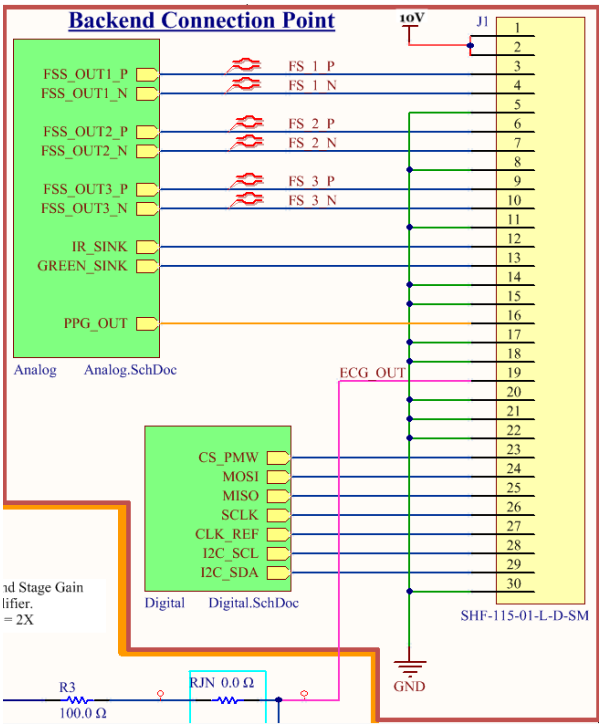

Figure 3.7: Diagram showing the ribbon cable connection wiring

3.3.3. Frontend to Backend Connection

The connection from the frontend to the backend is over a 30 pin flat ribbon cable of 1.27mm pitch. The signals over this cable have been spaced out to avoid cross talk between analog and digital signals. The wiring pattern is shown in 3.7. The ground wires act as passive shields between the signal pairs and keep them seperated. The differential pairs of Force sensor have one ground shield between them. The sensetive signals of ECG and PPG are surrounded by two ground wires each. Finally the digital and analog signals are kept apart as far as possible to prevent crosstalk.

3.3.4. Digital Sensors

The digital sensors in the system are the Accelrometer and the optical navigation sensor. The accelerometer is the MPU6050 [5] and communicates over I2C. Moreover a reference clock signal from the MUSEIC V2 is used to synchronise the timings of measurenments to the MUSEIC V2

The second digital sensor in the system is the optical navigation sensor the PMW3306[6]. The sensor communicates over SPI. Each chip is individually addressed by lowering its Chip Select (CS) lines. The chip select lines are controlled by two GPIO pins that are controlled by the firmware.

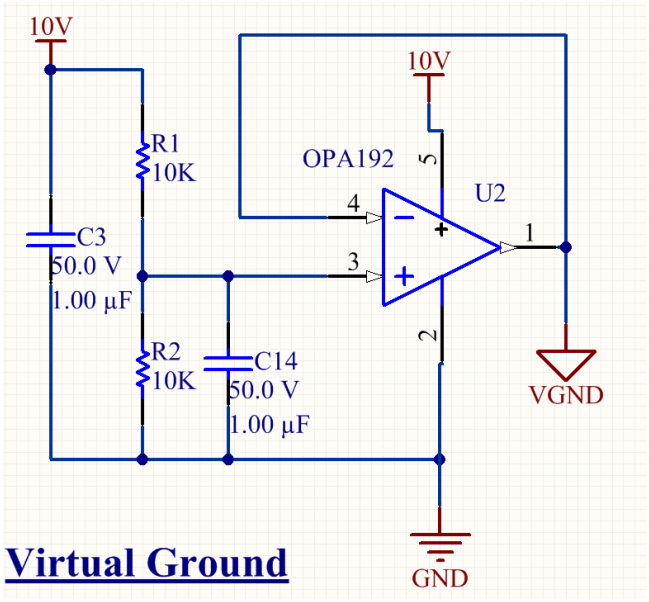

Figure 3.8: The virtual ground circuit.

3.3.5. Force Sensors

The analog sensors connect to the MUSEIC V2. The force sensors are maximum 3.3V and need to be steped down to 1.2V. Moreover the six inputs from the two electrodes are multiplexed into 3 outputs due to the limitations of reconfigurable channels in MUSEIC V2. The signal from the front end is first stepped down to 1.2V rail using buffered voltage dividers. While routing care was taken to keep the differential pairs as close as possible before and after the step down. After stepping down the signal the signals pass to a 6 channel 2:1 multiplexer. The normally open input of the multiplexer connect the signals coming from the left electrode and the normally closed side connect the right electrode. The multiplexer output goes to the analog input channels of the MUSEIC V2.

3.3.6. ECG

The ECG analog design for the non-contact ECG has been borrowed from the imec non-contact group V3.1 system. For dry-contact ECG the design consists of a a single unity gain buffer. A pair of 0Ω resistances select which mode the electrode will act in by bypassing the circuit of the other one.

Active Electrodes

The MAR frontend has active electrodes. This means that the ECG signals are buffered and amplified before transmission. This is done to overcome signal decay and cable artefacts. The buffer is a unity gain buffer charctherized by high input impedence and low bias current this is a requirenment of non-contact systems[40]. A passive 0.48Hz RC high pass filters to remove Direct Current (DC) noise and finally a second stage gain factor 2 amplifies the signal before transmission.

Virtual ground

The dual power supply for the system is between +5V to -5V. The supply to the front end is single sided 10V. A virtual ground for the circuit is genrated through a buffered voltage divider circuit. The voltage divider is implemtned three times in the design one at the backend and once for each of the two electrode. This ensures a stable mid-supply voltage that is independant of voltage drop across the cables. The voltage divider uses 2 $10K\Omega$ resistances and a OPA192 amplifier for a buffer. The circuit diagram for it is shown in 3.8

When the system is used in dry contact mode the Body Bias is generated from MUSEIC V2, when used in non-contact mode the DRL is generated on the backend. Both Body Bias and DRL are connected through the body through Ag/Cl electrodes to minimize motion artefact noise from them.

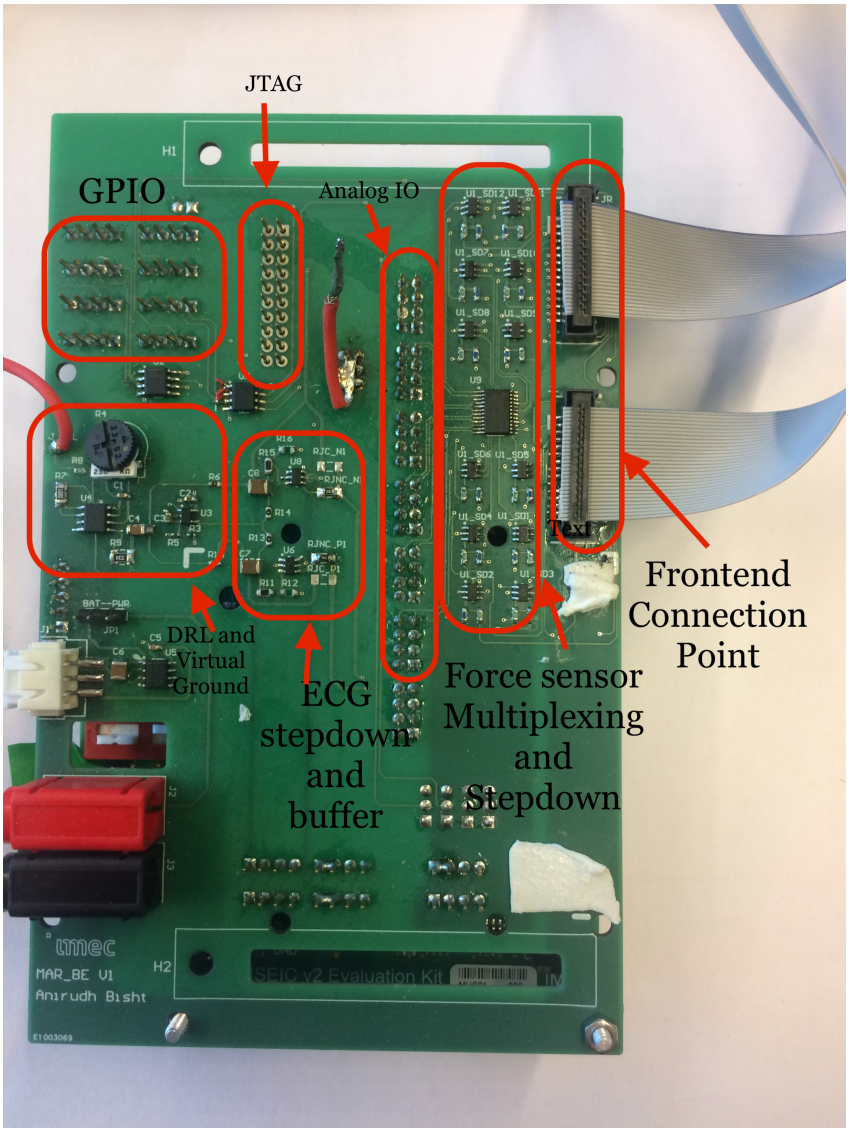

Figure 3.9: Top of the assembled backend showing showing the various sub-circuits.

4

Firmware Design

The firmware for the system runs on imec's MUSEIC V2 platform. The platform has a Cortex M0+ ARM processor. The firmware implements Cortex Microcontroller Software Interface Standard (CMSIS) framework for low level hardware access. A functional block diagram of the chip is show in 4.1 As seen in functional block diagram the core, memory bank, DMA are connected over the high speed AMBA High-performance Bus (AHB) bus. Peripherals including the SPI,I2C, timers and other low speed peripheral on the chip communicate on a Application Peripheral Bus (APB).

Configurations and data from these peripherals is accessed through memory mapped I/O. Memory mapped I/O is a way of communicating to external peripherals when they are located on a specific memory address[1]. Access to certain memory locations thus access data on these peripherals. Pointers to these memory locations can be modified to change the configuraiton of the peripherals and read and write to them.

MUSEIC V2 drivers abstract away these low level memory mapping and pointer creation, instead they exposes functions for access to different peripherals and manage word alingment for all read and write operations.

4.1. Configuring peripherals

When the firmware is loaded the first steps are to initialise all the required peripherals to their correct settings for operation.

4.1.1. Clock

The first peripheral to be configured is the clock. The MUSEIC starts code execution in a default clock configuration, t There is a 32Khz reference clock that acts as input to the MUSEIC V2 Phase Locked Loop (PLL), from this reference we use clock multipliers of 310 to achieve the desired clock speed of 10Mhz.

4.1.2. GPIO Multiplexer

As disucssed in 3.3.1 the GPIO pins of the MUSEIC V2 are organized as groups of four pins. Each group can perform a specific function, this ranges from being a acgpio or I2C,SPI or Universal Asynchronous Receiver-Transmitter (UART). The configuration can be changed by changing the value of the configuration register of each group. We thus select our desired configuration to match our hardware design.

4.1.3. I2C and Accelerometer

We enable two different I2C buses and map them to differnt GPIO groups. This allows conflict free access to the MPU-6050 as they have the same address. The configurations to the MPU6050 are written to disable its sleep state, and enable accelrometer reading.

Each loop iterations 12 bytes are read from the sensor into the buffer. These 12 bytes are read sequentially from the starting address of 0x3B. They read the three axes information from the accelrometer, and 2 axes of the gyroscope.

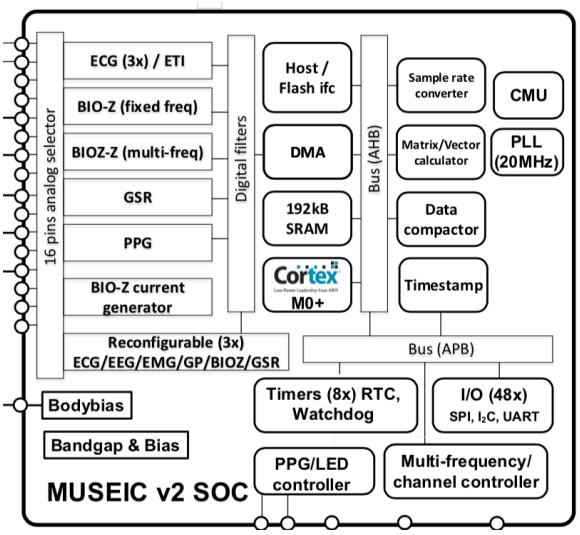

Figure 4.1: The MUSEIC V2 overview block diagram, taken from MUSEIC V2 datasheet, internal document [9]

4.1.4. SPI and Optical Navigation Sensor

The SPI bus is initated for communicating with the optical navigation sensor. Two GPIO pins in a seperate group are also instantiated to act as CS lines for the left and right electrode. The timings for the SPI clock module is derived from the main clock. the 10Mhz clock is divided by 18 to achieve a 500Khz clock. This is four times slower than the maximum possible speed of 2Mhz supported by the chip but is a saftey margin taken to avoid clock jitter over long cables.

Initialising each chip individually consists of a uploading a firmware to its Static Read Only Memory (SROM), Configuring parameters for tracking, and finally putting the circuit in burst mode. Burst mode is a special way of communicating with the PMW3360 sensor that removes the overheads of address-data communication way of standard SPI.

In burst mode the PMW3360 sensor sends 12 bytes of fixed data every time it is polled. These 12 bytes contain the following tracking information

- Displacement measured in X and Y direction since last report, in terms of counts.
- Surface Quality is the number of features tracked by the DSP, can be used as an indicative value for the lift of the sensor and accuracy of displacemnt reading. A lower value corrosponds to a chip that is elevated and also reduces the accuracy of tracking.
- Maximum Minimum and Average value of pixel illumination. These values similar to the surface quality can be used to judge the quality of tracking. Large difference between the maximum and minimum pixel value indicate a good contrast on the tracking surface and hence leads to accurate feature tracking and displacement reports.
- Shutter configuration used by the sensor, A large change in contrast is compensated by the sensor by changing the value of its camera shutter. Changes in the shutter can cause large changes in the pixel values, even when no motion may have occured as the chip tries to better focus on the tracking surface.

4.1.5. Timers

MUSEIC V2 has 8 timers, they are 32 bit down-counter timers. Eight timers are grouped into two Nest Vector Interrupt Controller (NVIC) interrupts and their status bit can be used to find which timer fired in the interrrupt handler. Seven Timers are used in the current system as shown in 4.1.

Timer 1 controls the switching of the external multiplexer gpio pin. Timer 1 can switch this pin at a given frequency to enable capturing data from both sets of force sensors.

A communication override exists in code which allows the host to force one state on the GPIO. This override exists to enable continious reading from only one electrode during testing and during certain parts of the experiments. When this override is activated Timer 1 is disabled. Timer 1 interrupt also updates the state of

Timer Number	Purpose	Auto Reload	Timeout
0	Timestamp generator	No	34 minutes
1	Switching the External Multiplexer	Yes	31.25 msec
2	Managning timeout on host SPI	No	7 msec
3	Synchronised starting of AFEDMA	No	100 msec
4	Polling optical sensor	Yes	0.8 msec
5	Polling accelerometer 1	Yes	3.6 msec
6	Polling accelerometer 2	Yes	3.6 msec

Table 4.1: Timer Configurations and purpose

the external multiplexer register after it switching which is important for 4.2.1 code to mark the data packets correctly.

Timer 2 is controlled by the host communication module of the code. Timer 2 is started after a packet is sent from MUSEIC V2 to the host. After timer 2 expires it checks if the communication has completed from the host side. In the event the host misses the data packet or times out it will reset the communication channels to try again. Timer 2 timeout checking prevents the system from entering a deadlock.

Timer 3 is uniquely linked to the AFE DMA and when its interrupt fires it triggers the synchronised starting of all analog channels. For this purpose timer 3 is a one-shot timer that is started after all AFE channels have been configured. Moreover when the external multiplexer is switched the incoming data packets to channels 2,3 and 4 contain switching noise from the multiplexer. This data is thus discarded and the reconfigurable channels are reinitialised and timer 3 is reset to synchronise them again.

Timers 4, 5 and 6 are countdown timers that auto-reload. They are timers for intiating periodic communication to the external sensors The countdown time determines the frequency at which the sensor are polled. When a sensor is polled its marker is checked before reading and updated after a succesful read. The timers only initiate the reading of a sensor, the actual reading is managed by the controller, and memory writing is written by the DMA as discussed in 4.1.8

4.1.6. Timestamp Generator

Timestamp generator is a peripheral in MUSEIC V2 that can store 15 unique timestamps. These timestamps read from a common timer, in this firmware it is timer 0. Each timestamp module stores a timestamp when its configured interrupt fire. Timestamp linked this way are always accurate to the time of the arrival of the interrupt. Since every interrupt in the system can be used for synchronising a timestamp we can synchronise both external sensors using the bus interrupts and internal analog data packets using internal interrrupts. When analysing data from the system and finding correlation it is vital that the data be time synchrnoised. The timestamp generataor module ensures that the timestamps for the data packets are accurate and synchronised.

4.1.7. AFE

The AFE of the MUSEIC V2 is able to measure a wide range of bio parameters, including ECG,Bio Impedance (BIOZ),Galvanic Skin Response (GSR) and PPG. In addition it has three reconfigurable channels that can serve any general purpose functionality. The three reconfigurable channels are configured to read differential signals and serve as analog channels for the force sensor.

ECG

One of the three available ECG channels is used for measuring ECG. Each AFE channel comes with various configurable analog settings and digital filter banks. The analog configuration for the ECG channel selected are listed below are the ones that deviate from the default. The digital Configuration of the ECG channel includes configuration of a digital filter bank.

- Instrumentation amplifier gain of 70V/V

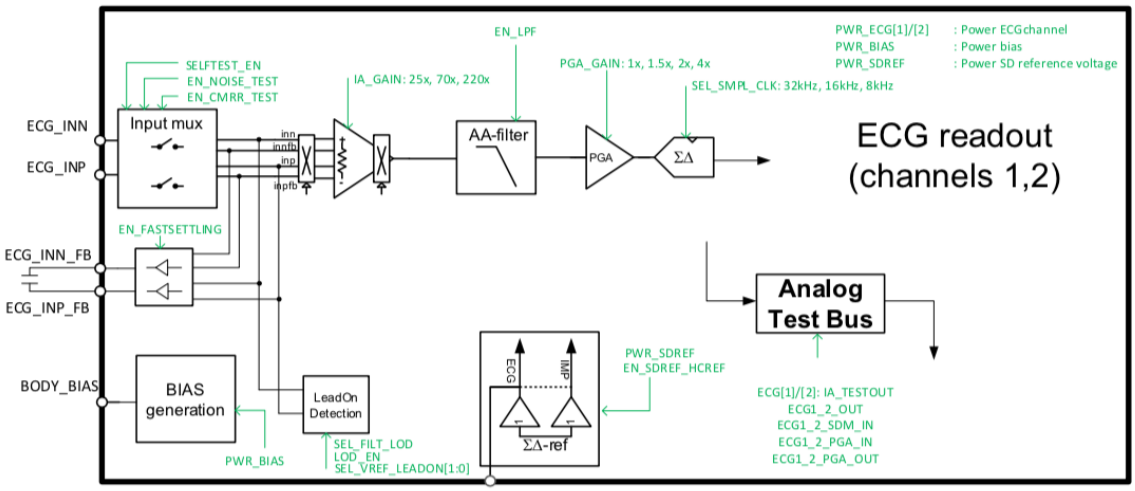

Figure 4.2: The internal of the ECG analog block of MUSEIC V2 taken from MUSEIC V2 datasheet internal document [9]

- Post Gain Amplificaiton of 1V/V
- ADC sampling rate of 32KHz
- CIC filter decimation of 64, effective sampling rate of 512Hz
- Accumalator bypassed
- 40 Hz digital lowpass filter

Force sensor Reconfigurable channel
Simlarly for the force sensor channel we have the following configurations

- Instrumentation amplifier gain of 1V/V
- Post Gain Amplificaiton of 2V/V
- Low Pass filter of 300Hz cut-off frequency
- ADC sampling frequency of 4Khz
- CIC filter decimation of 16, effective sampling rate of 512Hz
- 40Hz lowpass filter

These settings were changed during the tests and not all data collected follows the same configuration. In particular the sampling rate has to be adjusted to keep data flow constant.

4.1.8. DMA

There are two DMAs present in MUSEIC V2. The 17 channel pl230 DMA is used for communication between the host, Static RAM (SRAM) and peripherals. The second is an Analog DMA that stores data from the analog channels to the SRAM. The configuraiton for pl230 DMA are described in [10] documentation. For the purpose of this firmware there are four channels of the pl230 dma used. These channels are for the host SPI communication, the SPI reading from the optical navigation sensor and I2C data reading from the accelerometer to the SRAM. The configuration of these channels can be seen in 4.2

DMA channel	Iterations per cycle	Source alingment	Source increment	Destination alingment	Destination increment
Host SPI	256	Word	Word	Word	Fixed
Optical Navigation SPI	12	Byte	Fixed	Byte	Byte
Accelerometer I2C	2	Word	Fixed	Word	Word

Table 4.2: Configuration of the pl230 DMA channels

4.2. Data Transfer

4.2.1. Tracking Data Channels

The memory allocated for storing data from the sensors is organzied into buffers. These buffers store data from the various sources. Each sensor source is termed a channel. Channel Markers maintain the state of each buffer. Each data buffer is 256 words or 1024 bytes long. Each sensor writes to two buffers, this two buffer system allows us to write to one buffer while the second buffer is ready to read. This prevents race condition where data might be read and written to at the same time, and also allows continious writing to a data stream.

Analog channels maintain two buffers, the channel marker is a 3 bit value. Bit 0 and Bit 1 determine if buffer 1 and 2 are ready to read from. Bit 2 is used to check if a channel is dirty.

Dirty channel is used for marking reconfigurable channels after the external multiplexer switches. Once a channel is marked dirty the data stored in the data buffer is discarded.

For Digital channels the channel marker maintains a count of how many samples of data have been written to the buffer. Once the counter reaches limit for the buffer the channel is marked ready. Digital channles maintain a data flow wherein the transfer of data from peripheral to memory is triggered by its timer. The flowchart4.3 demonstrates the flow of control of a channel as the timer intiates a read to the peripheral, the data is read by a DMA channel and added to the buffer and finally a filled buffer is sent to the host via another DMA transfer.

4.2.2. Identifying Data Packets

The first word of a buffer is called a channel signature. A channel signature is a unique identification for each channel, this allows the host to identify each data packet and know which sensor it belongs to. The first six bits of the word identifies the channel and the remaining 26 bits holds the timestamp. The first two bits is 0b11 for analog channel and 0b10 for digital channel. Further analog channel holds a 4 bit value. The highest bit is the position of the multiplexer position. The reamining 3 bits are the identity of the channel.

in digital channels all 4 bits hold the digital channel index.

4.3. Main Program loop

The main program loop runs infinitely. It starts after all sensors have finsihed configuring. The last peripherals to be configured are the timers. The start of the timers triggers the data capturing and storing cycles. Timer 3 to 6 start the synchronised collection of data from all channels.

The main loop manages the sending of data packets to the host pc. The packets are sent as and when their respective buffers are full. In each iteration of the loop we first check if the SPI channel to the host has finished, if this channel is busy no data can be sent and we are forced to wait. We loop through all the channels in a round robin fashion.

4.3.1. Round Robin

In the round robin loop each channel is checked if it is ready to transmit. When a channel is found to be ready, the following steps are taken.

1. The data header of the channel is stamped as explined in 4.2.2
2. Channel 0 of the pl230 DMA is triggered to start the memory transfer to the SPI controller.
3. The host SPI channel is configured for a transfer.

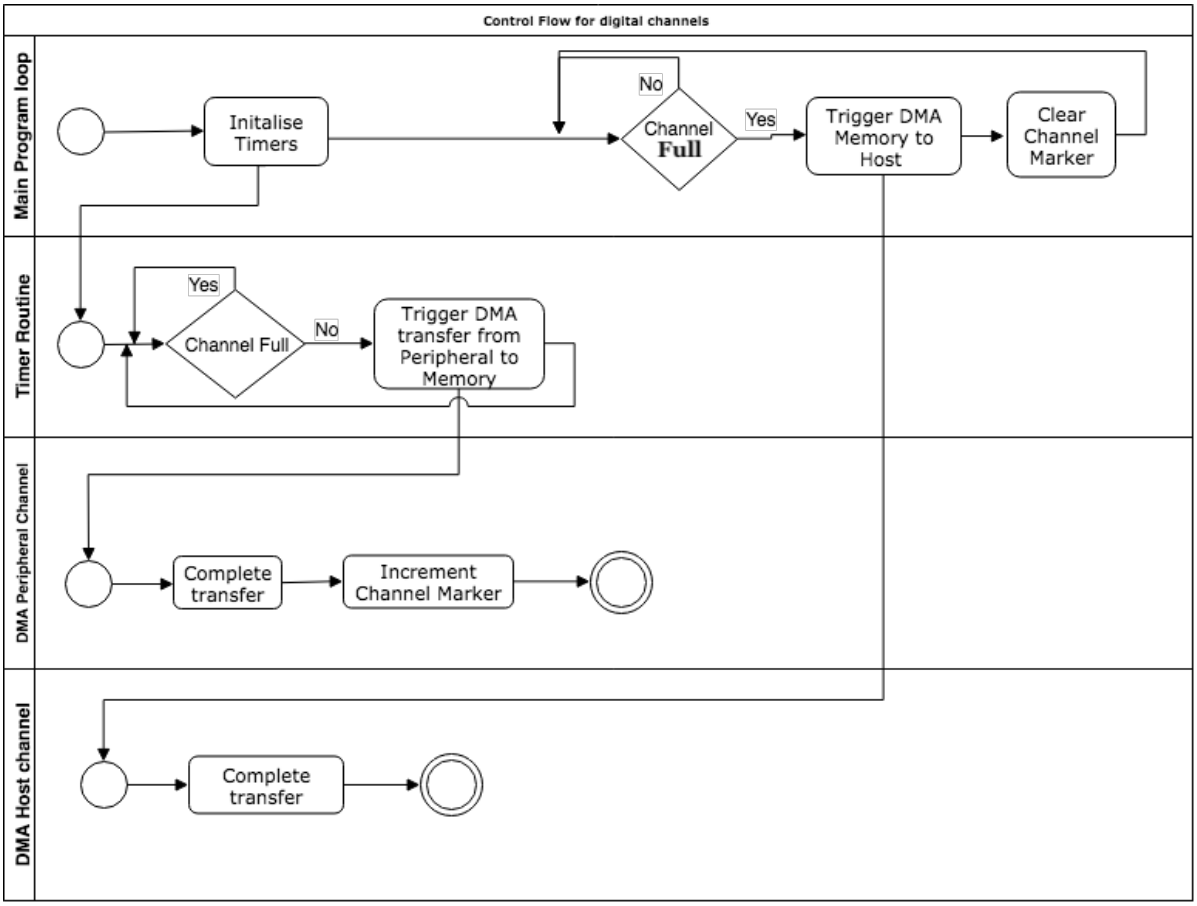

Figure 4.3: Flowchart showing the flow of control on a digital channel, with synchronisation of next tast being maintained by the channel marker

4. The Ready to Read pin is lowered to signal to the host to start a read.

5. The SPI channel timeout timer is activated, if it reaches zero the transfer is aborted.

6. The channel marker for the channel is cleared and the flow of control exits the current loop cycle and waits for the host communication to finish.

4.4. Host Python Scripts

The python script on the host side uses the CP2130 drivers and acts as the master for the host spi connection.

A Ready-to-read pin signals script that data is available to be read. Each iteration it reads a fixed number of bytes from the sensor which will alawys include one data packet.

The data packets are identified using the headers, the data packets are split into individual samples. The individual samples are timestampped by interpolating the timestamp from the header, and sampling rate of the sensor.

Next the data is written to a Common-separated Values(csv) file and also sent to the Graphaical User Interface controller for live plotting. Due to the large overhead of writing to the file of closing and opening the file it is more efficient to write the data in large bursts. To achieve this the data to be written is stored in an array.

Once the array fills to its threshold lenght a burst write to the file is initiated in a seprate thread to keep the reading thread running. The threshold of this lenght is dependent on the execution platform and also the configured clock settings of the CP2130.

5

Measurement and Results

This chapter will showcase the results from the MAR. The data generated from the system is stored in Comma-Seperated Values (CSV) files for analysis. For the purpose of data analysis MATLAB has been used, a set of scripts have been developed that read data from the stored files and plot data showcasing the response of each sensor against the ECG signal, synchronised by timestamp.

Due to limitations of time only the force sensor and optical navigation sensor were properly analyzed and can be discussed. Data from the MPU-6050 sensor was collected but has not been filtered and analyzed, this was given a low priority due to the existing body of work that has already been done using this sensor. However there is potential in the data from the MPU-6050 being useful as an augmented sensor for future algorithms that can track motion artefacts using a mult-modal approach.

Initial tests of the system were done on the author and were used to verify the functaionlity and integrity of the system. They also validated the use of timestamps for synchronising data and established the overall data flow.

Later the system was tested on ten subjects at the Holst Center in a internal study.

The results of those tests lead the way for imporvenments in the system design. There was data collection performed on the author again after these imporovenments had been made and are part of the final results.

5.1. ECG signal quality

The ECG signal captured by the system is not comparable to a clinical measurenment of ECG, however the morphological information of T-waves and the QRS complex are clearly distinguishable. The drop in signal quality is most likely due to the long cable artefacts, presence of digital and analog signals in close proximity, and a lack of active shielding on the cables.

While using the system in non-contact mode adjustment of the DRL gain plays an important role in obtaining usable ECG signals. Non-contact system can suffer from very high signal distortion if the DRL is not properly tuned. This tuning can change from subject to subject and also be affected by the ambient noise in the environment. As a personal annecdoate the system was mostly tested on a workbench that also had a laptop, removing the laptop from its power supply was important to maintain signal quality over experiments.

5.2. Testing Protocol

After the system had been sufficiently tested to be proven to work it was tested on other human subjects.

The testing protocol was designed to study the affect of local and generic motion aretfacts. The experiemnts were divided into threee distinct phases and were performed twice for each subject, first with dry-contact electrodes and next with non-contact.

The three phases are described below.

The first phase was to gather reference data for the system. The subjects were asked to sit still and breathe normally.

The second phase aimed at measuring local motion artefacts. The subjects were asked to make predefined motions local to one of the electrode. These motions were aimed at creating the following artefacts.

- Push-pull artefacts. By pushing down the electrode, holding the push and then releasing it.

- Lateral Motion Artefacts. Move the electrode left and right and up and down over the body in short motions, giving rest between each motion.

- Skin Stretching Artefacts. Stretching and rotation of arm to stretch the skin under the electrode.

Push-pull artefacts are commonly discussed in literature when discussing motion artefacts.[40] The skin stretching artefacts were induced by moving the arm near the electrode as that stretchies the skin. This was done to induce skin stretching artefacts as discussed in [43]. The final phase of the experiment was performing generic movenments including sitting, standing, walking and doing stretching exercises.

During the experiments the electrodes needed to be held in place due to the lack of adhesive in them, a velcro belt was used to achive this. The Graphical User Interface (GUI) used during the experiments allows for the recording of timestamps from the system, these timestamps could be used to create a table showing the start and end time of the different experiment phases and events. This can be used to quickly find the required event in post-analysis.

5.3. Motion Artefacts

This section we will discuss the different motion artefacts as captured by the system.

5.3.1. Push-pull Artefacts

Data for push-pull artefacts is gathered during phase 2 of the testing protocol. Non-contact system has a lower resilience to artefacts and shows large deviations in the signal in the range of 300-400mV peak-peak oscillations. These oscillations swing far above the signal peak-peak of 50mV.

Moreover the bandwidth of the signals eclipses the signal spectrum. Dry-contact electrodes perform better in terms of resilience to artefacts.

The force sensor functions as a good SQI indicator for these artefacts, while the signal itself does not correlate in the morphological sense to the artefacts. The termporal correlation of change in force sensor reading to onset of motion artefacts exists. The current experiment setup due to the presence of the velcro

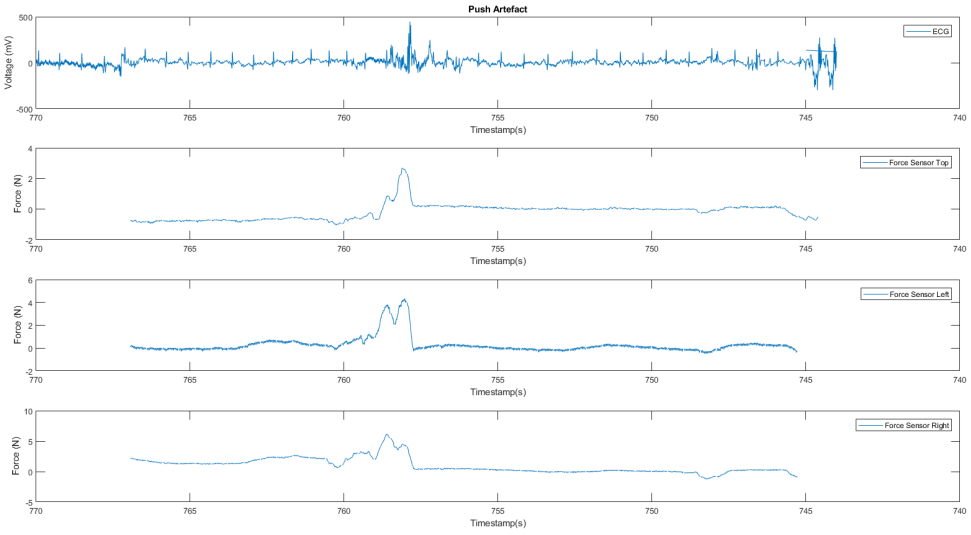

Figure 5.1: A Push artefact as captured by the ECG channel time synchrnoised to the three force channels of the affected electrode

belt that held the electrodes against the chest the force sensors were near saturation. Theis is visible as the sharp saturation of the force under strong push artefacts.

However force sensor is not unique in being able to measure push-pull artefacts.

The parameters of the AFE channels were adjusted to prevent the signal from saturating during artefacts. This gives us a chance to observe the signal or

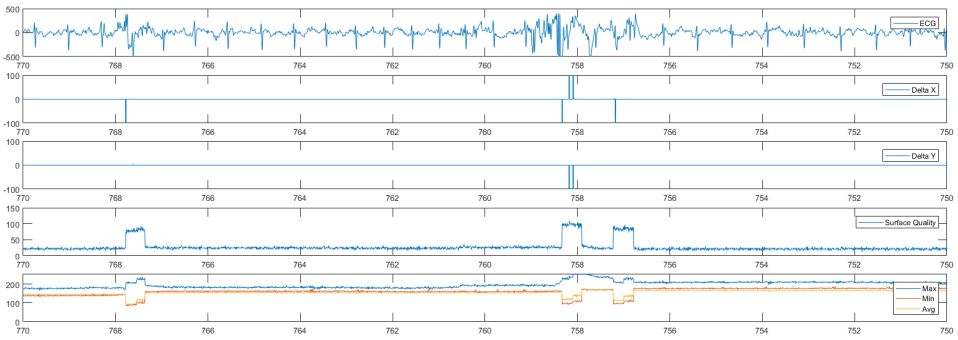

Figure 5.2: Push artefacts as measured by the optical navigation sensor

5.3.2. Breathing Artefacts

After the enhancemnt to the firmware as discussed in 5.4 the optical navigation sensor has increased accuracy. This increased accuracy allows surface quality to capture breathing motions during

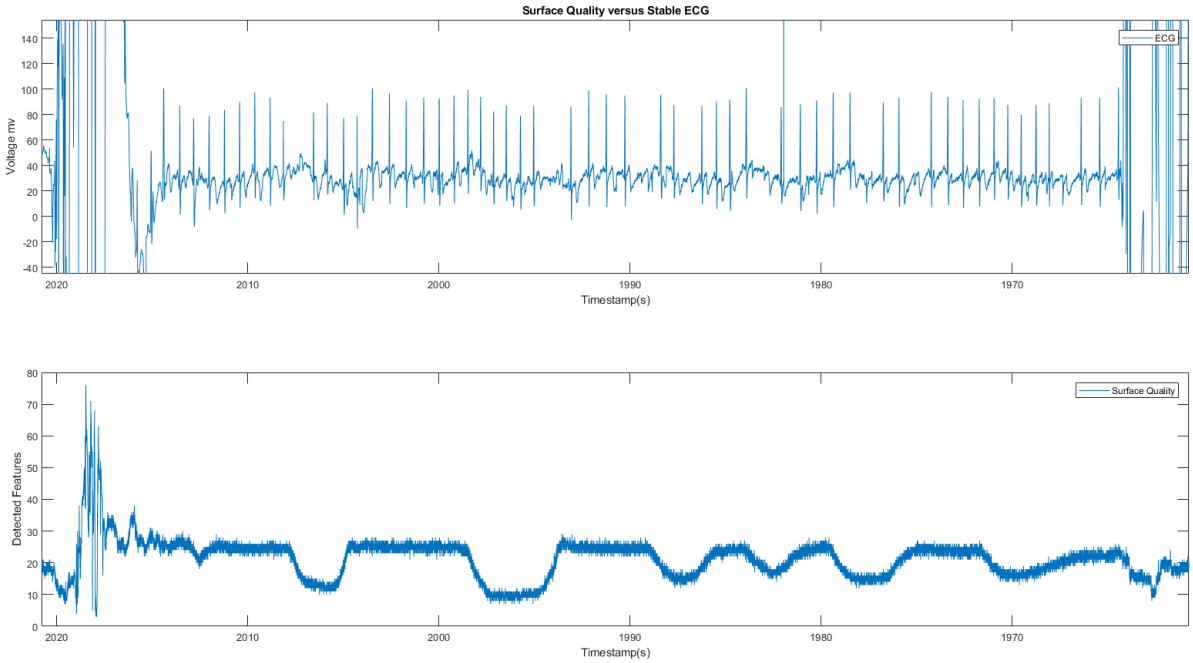

Figure 5.3: Breathing motion as captured in Surface quality.

5.3.3. Lateral motion artefacts

Lateral motion artefacts are charachterized as the ones that occur during the motion of the electrode in the plane parallel to that of the skin surface. In dry-contact measurement this is the motion between the electrode and the skin. Due to the adhesion between the electrode and the skin, along with the force applied by the velcro belt, lateral motion becomes restricted. In non-conatct the lateral motion is over the textile surface of the clothing. If allowed to move freely the lateral motion creates motion artefacts of very high peak oscillations.

The affect of lateral motion is more profound on the non-contact electrodes compared to the dry contact electrodes. The voltage swing for non-contact usually saturates the output, while dry-contact the signal does not saturate, and the peaks are still recoverable in the motion artefact noise. This comparison is shown in 5.4

In non-contact electrodes the lateral motion creates oscillation peaks that decay to the normal baseline over time after the motion stops. Aggresive highpass filtering in this region can recover peaks as shown in 5.5

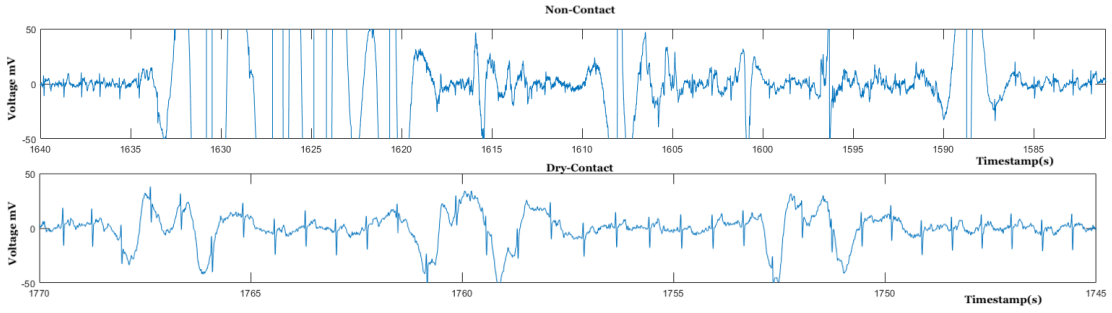

Figure 5.4: Comparison of laterla motion artefacts

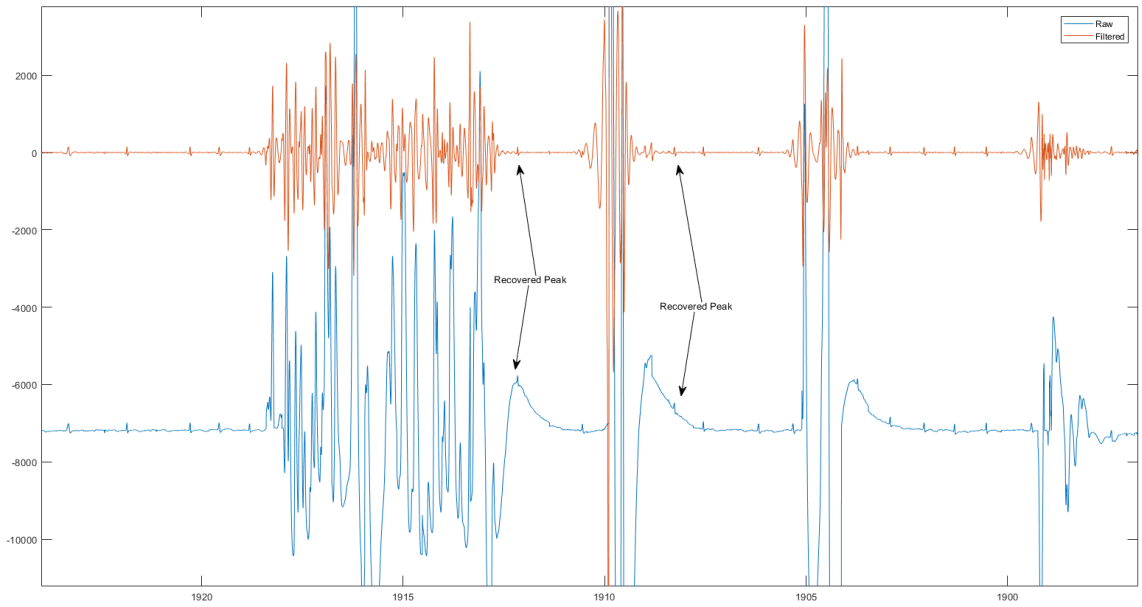

Figure 5.5: Comparison of the signals.

While the optical navigation sensor is more suited for measuring lateral motion, the force sensor is also sensetive enough to measure them. Lateral motion in the force sensor shows as oscilation during the motion phase. There does not seem to be an indication of the direction of the motion.

5.4. Lateral motion non-contact firmware enhancement

For non-contact system lateral motion causes artefacts of high peak oscillations. These peaks correlate well to the peaks in the displacement readings of the optical navigation sensor. The Displacement is calulcated as the root mean square of the Delta-X and Delta-Y reading of the optical navigation sensor. From observation we can see that while peaks in the displacement measurenment and ECG signal, there are oscilations after each peak in the ECG.

This indicates that both the motion artefacts and motion signals are affected by strong impulse peaks when lateral motion between the electrode and surface occurs. When this impulse peak passes through the high pass filter it gets spread out into a smooth curve as the capcitor charges and discharges slowly.

5.4.1. Simulink Model for Signal Mutation

Since the digital signal from the optical navigation sensor is not affected by the high pass filter, a mutated signal can be derived by simulating the digital signal as a voltage that passes through the frontend circuit.

The frontend system is re-created in simulink to achieve this mutation. The signal is also filtered through a median filter of a sliding window lenght of 25 this smoothes out the signal and filters out all the lone peaks.

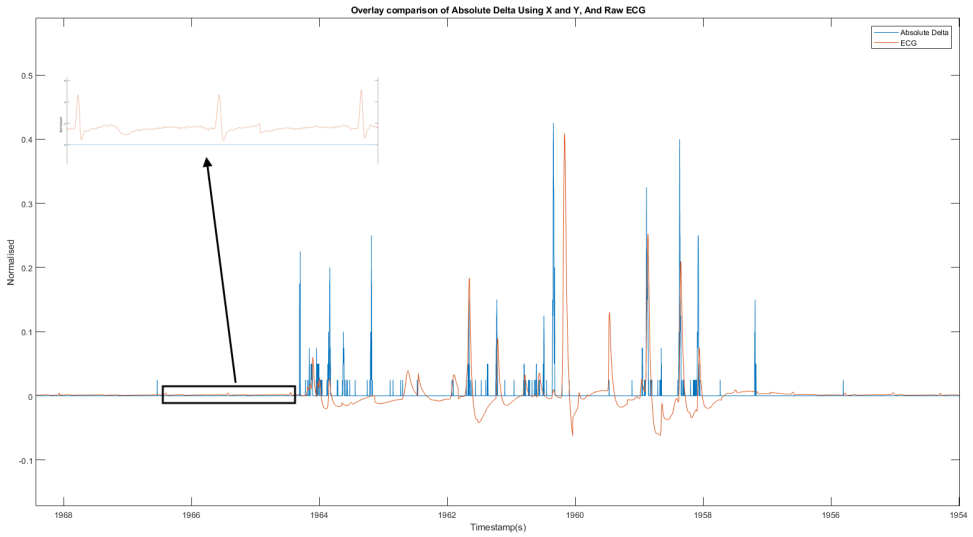

Figure 5.6: Correlation of ECG artefacts in non-contact, Overlay comparison of normalised value of both signals. Inset: Zoomed view of ECG signal.

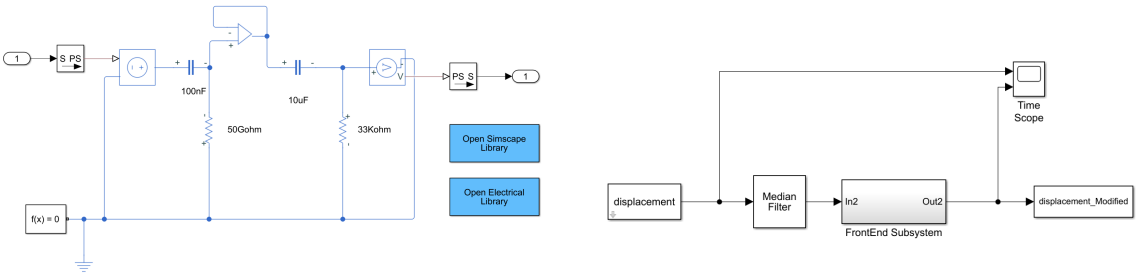

Figure 5.7: a) the recreated electrical frontend used for mutating the signal.b)Simulink model showing the overall flow, note the median filtering is done before the signal mutation.

The signal is passed through the model and the signal is mutated. After perofming signal mutation the cross correlation between the signals is calculated. For this first mutated signal is resampled to 512 Hz to match the frequency of the ECG signal.

The signals are alinged on a timestamp at the start of the event.

5.4.2. Correlation

To calculate the correlation between the signals, we first need to resample the data to match their frequency. Moreover since data are measured in different dimensions, the optical navigation sensor measuring counts of movenment and ECG in Volts, we normalise the data to make a comparison. The normalisation is done by the following formula for a given signal x[n].

$$\begin{aligned} mean_x &= \frac{\sum_{n=1}^{N} x[n]}{N} \\ x[n] &= \frac{x[n] - mean_x}{max(x)} \end{aligned} \tag{5.1}$$

The correlation is done using MATLABs cross-correlation function $xcorr$.[11]

5.5. Spectrogram analysis

Spectrogram analysis is the short-duration Fast Fourier Transform (FFT) over time of the signal. This allows visuvalisation of the changning frequency of the signal at the onset of motion artefacts dominate the spectrum. Due to high temporal correlation of the force sensor signals and the optical navigation signal to these motion artefcats they form effective metrics for SQI of the ECG.

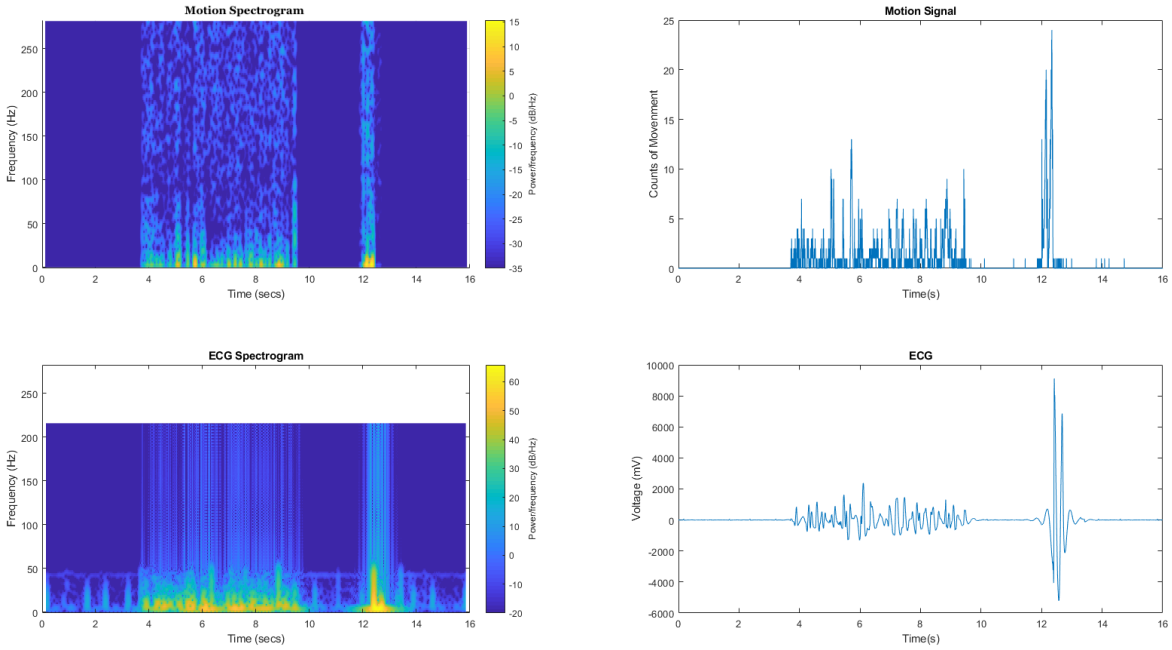

Figure 5.8: Spectrogram and time analysis of Displacement signal and ECG

6

Conclusion

6.1. Significance

In this thesis the design and validation of the MAR system has been shown. The system was designed with the goal to find an sensor that can be used as a reference for motion artefact noise in ECG measurenments. The optical navigation sensor and force sensor show great promise as auxillary sensors in dry-contact and non-contact electrode, as they have proven effective SQI indicators to measure the onset of motion artefacts. Moreover the optical navigation sensor shows great promise in its ablity to track motion artefacts and correlates well to the noise signal.

Given the limitations of the system to be implemented using off-the-shelf electronics some sensors are being used in unconventional ways, for example the use the optical navigation sensor for measuring the stretching. However the MAR system gives insight into which physical parameters we can try and capture to find their correlation to the motion artefacts.

6.2. Future Work

The system described in this thesis has not been designed from a product point of views, and even as a prototype it has room for improvenment. The architecture design of a backend and frontend system arose from the time constraint to make a system that also reamined relatively easy to debug. the MUSEIC V2 system can also be used in its more smaller SIRIUS package[9]. This will allow the digitisation of the signals closer to the body and remove a great deal of cable artefact nosie.

Morevoer data analysis of the acquired signals requires a proper investigation study for validating the results with the higher accuracy tracking of the optical navigation sensor. The optical navigation sensor in its current form hides a lot of information that is calculated internally by the DSP. This information could be a useful in finding better correlation metrics against the motion artefacts.

Moreover this thesis while implementing multiple sensors, does not utilize them in a multi-modal approach towards filtering. That will possibly require development of algorithms or machine learning approaches that fall outside the scope of this work.

Bibliography

[1] Arm devleoper page on memory mapped i/o. URL https://developer.arm.com/products/software-development-tools/ds-5-development-studio/resources/tutorials/accessing-memory-mapped-peripherals.

[2] Cp2130 by silabs. URL https://www.silabs.com/products/interface/usb-bridges/classic-usb-bridges/device.cp2130.

[3] Linear potentiometer transducer working explanation. URL http://www.instrumentationtoday.com/linear-potentiometer-transducer/2011/07/.

[4] Medcat connectors for ecg. URL http://www.medcat.nl/.

[5] Mpu6050 by invensense a popular accelrometer. URL https://www.invensense.com/products/motion-tracking/6-axis/mpu-6050/.

[6] Pixart manufacturer of optical navigation sensor. URL http://www.pixart.com/.

[7] St time of flight sensor. URL https://www.st.com/en/imaging-and-photonics-solutions/vl53l0x.html.

[8] Cardiovascular diseases. URL http://www.who.int/cardiovascular_diseases/en/.

[9] imec, museic documents are internal documents of imec. URL https://www.imec-int.com/en/system-on-chip.

[10] Arm documentaiton on the primecell pl230 dma controller. URL http://infocenter.arm.com/help/topic/com.arm.doc.ddi0417a/DDI0417A_udmac_pl230_r0p0_trm.pdf.

[11] Cross correlation function xcorr in matlab. URL https://nl.mathworks.com/help/signal/ref/xcorr.html.

[12] Kalra A and Lowe A. Quantifying skin stretch induced motion artifact from an electrocardiogram signal-a pilot study. *Journal of Biosensors & Bioelectronics*, 7(2), 2016. doi: 10.4172/2155-6210.1000204.

[13] Mohammad J. Abu-Saude and Bashir I. Morshed. Patterned vertical carbon nanotube dry electrodes for impedimetric sensing and stimulation. *IEEE Sensors Journal*, 15(10):5851–5858, oct 2015. doi: 10.1109/jsen.2015.2449301.

[14] AHF. What is afib„ 2016. URL https://www.heart.org/en/health-topics/atrial-fibrillation/what-is-atrial-fibrillation-afib-or-af.

[15] Thanit Apiwattanadej, Li Zhang, and Holden Li. Electrospun polyurethane microfiber membrane on conductive textile for water-supported textile electrode in continuous ECG monitoring application. In *2018 Symposium on Design, Test, Integration & Packaging of MEMS and MOEMS (DTIP)*. IEEE, may 2018. doi: 10.1109/dtip.2018.8394190.

[16] Ibrahim Baggili, Jeff Oduro, Kyle Anthony, Frank Breitinger, and Glenn McGee. Watch what you wear: Preliminary forensic analysis of smart watches. In *2015 10th International Conference on Availability, Reliability and Security*. IEEE, aug 2015. doi: 10.1109/ares.2015.39.

[17] Noel Carroll. Key success factors for smart and connected health software solutions. *Computer*, 49(11): 22–28, nov 2016. doi: 10.1109/mc.2016.340.

[18] Mahesh Chavan, Ra Agarwala, and Mahadev Uplane. Suppression of noise in the ecg signal using digital iir filter. 01 2008.

[19] Yu Mike Chi, Tzyy-Ping Jung, and Gert Cauwenberghs. Dry-contact and noncontact biopotential electrodes: Methodological review. *IEEE Reviews in Biomedical Engineering*, 3:106–119, 2010. doi: 10.1109/rbme.2010.2084078.

[20] L. Citi, C. Olariu, and R. Barbieri. A lightwave client for semi-automated annotation of heart beats from ecg time series. In *2015 Computing in Cardiology Conference (CinC)*, pages 605–608, Sept 2015. doi: 10.1109/CIC.2015.7410983.

[21] B. Feddes, L. Gourmelon, M. Meftah, and T. Ikkink. Reducing motion artefacts of capacitive sensors. In *2007 29th Annual International Conference of the IEEE Engineering in Medicine and Biology Society*, pages 1532–1532, Aug 2007. doi: 10.1109/IEMBS.2007.4352593.

[22] Valentin Goverdovsky, David Looney, Preben Kidmose, and Danilo P. Mandic. Multimodal physiological sensor for motion artefact rejection. In *2014 36th Annual International Conference of the IEEE Engineering in Medicine and Biology Society*. IEEE, aug 2014. doi: 10.1109/embc.2014.6944193.

[23] Nejat Guzelsu, John F. Federici, Hee C. Lim, Hans R. Chauhdry, Art B. Ritter, and Tom Findley. Measurement of skin stretch via light reflection. *Journal of Biomedical Optics*, 8(1):80, 2003. doi: 10.1117/1.1527936.

[24] P.S. Hamilton and M.G. Curley. Adaptive removal of motion artifact. In *Proceedings of the 19th Annual International Conference of the IEEE Engineering in Medicine and Biology Society. 'Magnificent Milestones and Emerging Opportunities in Medical Engineering' (Cat. No.97CH36136)*. IEEE. doi: 10.1109/iembs.1997.754531.

[25] J. Heikenfeld, A. Jajack, J. Rogers, P. Gutruf, L. Tian, T. Pan, R. Li, M. Khine, J. Kim, J. Wang, and J. Kim. Wearable sensors: modalities, challenges, and prospects. *Lab on a Chip*, 18(2):217–248, 2018. doi: 10.1039/c7lc00914c.

[26] Rahul Kher, Tanmay Pawar, and Vishvjit Thakar. Combining accelerometer data with gabor energy feature vectors for body movements classification in ambulatory ECG signals. In *2013 6th International Conference on Biomedical Engineering and Informatics*. IEEE, dec 2013. doi: 10.1109/bmei.2013.6746974.

[27] Yoshifumi Kishimoto, Yasunari Kutsuna, and Koji Oguri. Detecting motion artifact ECG noise during sleeping by means of a tri-axis accelerometer. In *2007 29th Annual International Conference of the IEEE Engineering in Medicine and Biology Society*. IEEE, aug 2007. doi: 10.1109/iembs.2007.4352878.

[28] Eralp Kolağasioğlu. Energy efficient feature extraction for single-lead ecg classification based on spiking neural networks. Master's thesis, TU Delft, 2018.

[29] Fred M. Kusumoto. *ECG Interpretation: From Pathophysiology to Clinical Application*. Springer US, 2009. doi: 10.1007/978-0-387-88880-4.

[30] Nadine R Lang, Matthias Brischwein, Erik Hasslmeyer, Daniel Tantinger, Sven Feilner, Axel Heinrich, Heike Leutheuser, Stefan Gradl, Christian Weigand, Bjoern Eskofier, and Matthias Struck. Filter and processing method to improve r-peak detection for ECG data with motion artefacts from wearable systems. In *2015 Computing in Cardiology Conference (CinC)*. IEEE, sep 2015. doi: 10.1109/cic.2015.7411061.

[31] Yan Liu and Michael G. Pecht. Reduction of skin stretch induced motion artifacts in electrocardiogram monitoring using adaptive filtering. In *2006 International Conference of the IEEE Engineering in Medicine and Biology Society*. IEEE, aug 2006. doi: 10.1109/iembs.2006.260006.

[32] Luca Maiolo, Francesco Maita, Andrea Castiello, Antonio Minotti, and Alessandro Pecora. Highly wearable wireless wristband for monitoring pilot cardiac activity and muscle fine movements. In *2017 IEEE International Workshop on Metrology for AeroSpace (MetroAeroSpace)*. IEEE, jun 2017. doi: 10.1109/metroaerospace.2017.7999578.

[33] Satria Mandala and Tham Cai Di. Ecg parameters for malignant ventricular arrhythmias: A comprehensive review. *Journal of Medical and Biological Engineering*, 37(4):441–453, Aug 2017. ISSN 2199-4757. doi: 10.1007/s40846-017-0281-x. URL `https://doi.org/10.1007/s40846-017-0281-x`.

[34] C. Pylatiuk, M. Muller-Riederer, A. Kargov, S. Schulz, O. Schill, M. Reischl, and G. Bretthauer. Comparison of surface EMG monitoring electrodes for long-term use in rehabilitation device control. *2009 IEEE International Conference on Rehabilitation Robotics*, 2009. doi: 10.1109/ICORR.2009.5209576.

[35] M.A.D. Raya and L.G. Sison. Adaptive noise cancelling of motion artefact in stress ECG signals using accelerometer. In *Proceedings of the Second Joint 24th Annual Conference and the Annual Fall Meeting of the Biomedical Engineering Society] [Engineering in Medicine and Biology*. IEEE. doi: 10.1109/iembs.2002.1106637.

[36] M. G. Srinivasa and P. S. Pandian. Dry electrodes for bio-potential measurement in wearable systems. In *2017 2nd IEEE International Conference on Recent Trends in Electronics, Information & Communication Technology (RTEICT)*. IEEE, may 2017. doi: 10.1109/rteict.2017.8256600.

[37] Thomas J. Sullivan, Stephen R. Deiss, and Gert Cauwenberghs. A low-noise, non-contact EEG/ECG sensor. In *2007 IEEE Biomedical Circuits and Systems Conference*. IEEE, nov 2007. doi: 10.1109/biocas.2007.4463332.

[38] Leif Sörnmo, editor. *Atrial Fibrillation from an Engineering Perspective*. Springer International Publishing, 2018. doi: 10.1007/978-3-319-68515-1.

[39] Khawaja Taimoor Tanweer, Syed Rafay Hasan, and Awais Mehmood Kamboh. Motion artefact reduction from PPG signals during intense exercise using filtered x-LMS. In *2017 IEEE International Symposium on Circuits and Systems (ISCAS)*. IEEE, may 2017. doi: 10.1109/iscas.2017.8050418.

[40] Tom Torfs and Refet Firat Yazicioglu. Non-contact ECG recording system with real time capacitance measurement for motion artefact reduction. In *2013 IEEE Biomedical Circuits and Systems Conference (BioCAS)*. IEEE, oct 2013. doi: 10.1109/biocas.2013.6679657.

[41] T. Wartzek, R. Elfring, A. Janssen, B. Eilebrecht, M. Walter, and S. Leonhardt. On the way to a cable free operating theater: An operating table with integrated multimodal monitoring. In *2011 Computing in Cardiology*, pages 129–132, Sept 2011.

[42] T Wartzek, T Lammersen, B Eilebrecht, M Walter, and S Leonhardt. Triboelectricity in capacitive biopotential measurements. *IEEE Transactions on Biomedical Engineering*, 58(5):1268–1277, may 2011. doi: 10.1109/tbme.2010.2100393.

[43] John G. Webster. Reducing motion artifacts and interference in biopotential recording. *IEEE Transactions on Biomedical Engineering*, BME-31(12):823–826, dec 1984. doi: 10.1109/tbme.1984.325244.

[44] Bruce B. Winter and John G. Webster. Driven-right-leg circuit design. *IEEE Transactions on Biomedical Engineering*, BME-30(1):62–66, jan 1983. doi: 10.1109/tbme.1983.325168.

A

Device Safety Document

The following is the safety document of the MAR system as submitted in part to gain approval for testing. It highlights the safety of the sensors themselves for the patients and of the ECG channel with various redundancies. To note the references mentioned at the end of the document are of the this internal document not of the thesis.

ECG safety

The ECG electrodes for both Contact mode and Non-Contact mode include an input unity gain buffer with supply voltage tied to 10Volts [4]. This buffer insures high impedance on the patient side of the circuit. There is a third electrode for body bias that uses Ag/AgCl wet gel electrodes.

The IEC 60601-1 standard for maximum leakage and auxiliary currents to patients is taken for current limits. There are two different conditions of current mentioned as seen in [Figure 8] these are discussed in the following sections.

Leakage Current to earth

For all cases of the experiments the power will be provided from the onboard battery, the communication link will be made to a laptop that will be running on its battery power for the duration of the experiments hence removing all possibility of leakage current to earth.

Auxiliary Current

There are two cases for auxiliary current to the subject.

For Normal Case there is no danger of high current as the unity gain buffer on the ECG ensures a high input impedance, and limits bias current in the input side of circuit to 1pico-amperes max [4].

To tackle single fault condition i.e. when 10 Volts from the battery is shorts to input side of ECG on the electrode, a combination of resistor and capacitor is used to limit single fault current, this case simulation is shown in [Figure 1].

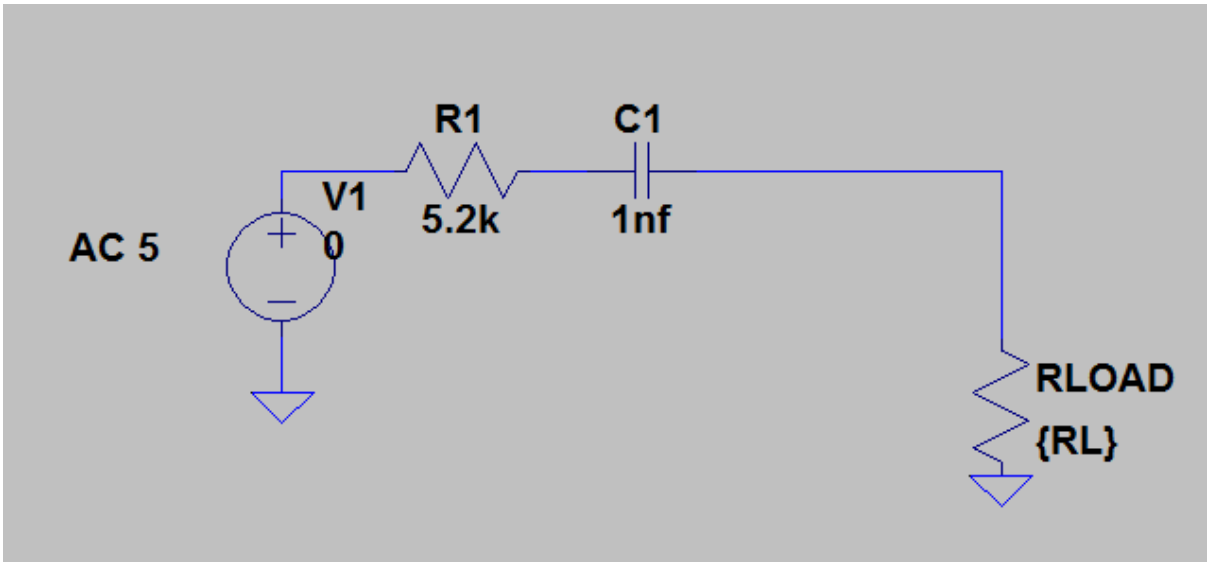

Figure 1 Simulation Circuit for single fault failure protection

A resistance of 5.2 KOhm and capacitor of 1nF are used. In accordance with IEC60601-1 current limits on human body these current limits are plotted in [Figure 2] and show that worst case fault current of this system fall below Type C(which is the strictest) fault current limits showing that the

system is Type C compliant.

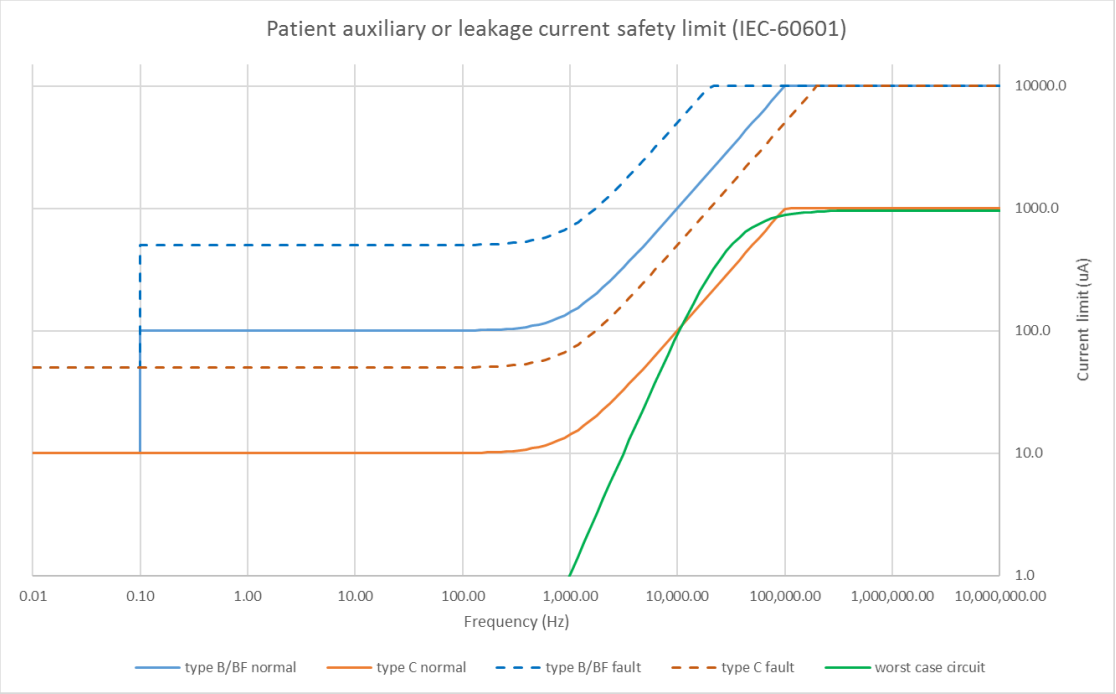

Figure 2 Frequency vs current for system worst case and IEC limits

The resistance in the simulation circuit is an addon to the existing circuit layout. To achieve this a bridge point was created on the PCB to accommodate two SMDs in the place of one. These changes are soldered and sealed hence is very difficult to bypass them during experiments.

To ensure proper resistance and capacitance values were soldered in this critical section the following steps were taken and changes for each electrode documented in the table below

1. Solder 5.5K ohm resistance and measure buffer to bridge point
2. Measure resistance from buffer input to bridge point and confirm it is ~5.5K Ohm
3. Solder 1nF capacitance from electrode contact point to Bridge point.
4. Measure resistance between bridge and electrode ensure it is open circuit
5. Test Electrode to acquire ECG signals
6. Plastic Seal top side of electrode.

Electrode ID	**Buffer To Bridge Resistance**	**Bridge to Electrode Resistance**	**ECG optainable**	**Plastic Sealed**
Non_contact-1	5.6K	Open Circuit	Yes	Yes
Non_contact-2	5.5K	Open Circuit	Yes	Yes
Contact-1	5.6K	Open Circuit	Yes	Yes
Contact-2	5.5K	Open Circuit	Yes	Yes

The electrodes for the dry-contact electrodes are finished with Ni/Au nickel gold finish. With a 3-6um of Nickel layer and 0.065 um to 0.1um of gold layer[5], and thus safe to use on skin.

The DRL(Driven right leg) circuit, used to reduce Common mode noise in non-contact ECG, a 100Kohm resistance is used to limit the output current to the body to 50 uA.

The Body bias used in contact mode is generated from MUSEIC.

Table 3 – * Allowable values of PATIENT LEAKAGE CURRENTS and PATIENT AUXILIARY CURRENTS under NORMAL CONDITION and SINGLE FAULT CONDITION

Current in µA

Current	Description	Reference	Measuring Circuit		TYPE B APPLIED PART		TYPE BF APPLIED PART		TYPE CF APPLIED PART	
					NC	SFC	NC	SFC	NC	SFC
PATIENT AUXILIARY CURRENT		8.7.4.8	Figure 19	d.c.	10	50	10	50	10	50
				a.c.	100	500	100	500	10	50
PATIENT LEAKAGE CURRENT	From PATIENT CONNECTION to earth	8.7.4.7 a)	Figure 15	d.c.	10	50	10	50	10	50
				a.c.	100	500	100	500	10	50
	Caused by an external voltage on a SIP/SOP	8.7.4.7 c)	Figure 17	d.c.	10	50	10	50	10	50
				a.c.	100	500	100	500	10	50
Total PATIENT LEAKAGE CURRENT [a]	With the same types of APPLIED PART connected together	8.7.4.7 a) and 8.7.4.7 h)	Figure 15 and Figure 20	d.c.	50	100	50	100	50	100
				a.c.	500	1 000	500	1 000	50	100
	Caused by an external voltage on a SIP/SOP	8.7.4.7 c) and 8.7.4.7 h)	Figure 17 and Figure 20	d.c.	50	100	50	100	50	100
				a.c.	500	1 000	500	1 000	50	100

Key
NC = NORMAL CONDITION
SFC = SINGLE FAULT CONDITION

NOTE 1 For EARTH LEAKAGE CURRENT see 8.7.3 d).

NOTE 2 For TOUCH CURRENT see 8.7.3 c).

* Total PATIENT LEAKAGE CURRENT values are only applicable to equipment having multiple APPLIED PARTS. See 8.7.4.7 h). The individual APPLIED PARTS shall comply with the PATIENT LEAKAGE CURRENT values.

Figure 3 IEC Leakage and auxiliary current guidelines

References

[1]FSS005 Honeywell force sensor https://sensing.honeywell.com/honeywell-sensing-force-sensors-fss-smt-product-sheet-008181-3-en.pdf

[2]PMW3360 Pixart Optical Motion Sensor http://www.pixart.com/upload/PMS0058-PMW3360DM-T2QU-NNDS-R1.30-06042016_20160902201411.pdf

[3]MPU6050 InvenSense Accelerometer and Gyroscope https://www.invensense.com/wp-content/uploads/2015/02/MPU-6000-Datasheet1.pdf

[4]LTC6240 Linear Technology Op-Amp http://www.analog.com/media/en/technical-documentation/data-sheets/624012fe.pdf

[5]Eurocircuit ENIG surface finsh https://www.eurocircuits.com/che-niau-or-enig-electro-less-nickel-immersion-gold/